LATE DARRIWILIAN (MIDDLE ORDOVICIAN) CONODONTS FROM EASTERN AND SOUTHEASTERN IRELAND

SVEND STOUGE, DAVID A.T. HARPER and MATTHEW A. PARKES

Abstract

The Middle Ordovician (upper Darriwilian) marine deposits of the Bellewstown Limestone Member and Tramore Limestone Formation in eastern and southeastern Ireland, respectively, yield a diverse conodont assemblage of 21 taxa. The sedimentary rocks deposited on the Bellewstown Terrane represent an intra-Iapetus island arc setting. The Tramore Limestone was deposited in a back-arc setting at the eastern margin of the Leinster-Lakesman Terrane that is considered part of the peri-Gondwanan Ganderia Terrane. The conodont assemblage, including species of *Baltoniodus*, *Eoplacognathus, Plectodina* and *Pygodus* is assigned to the *Pygodus serra* Conodont Zone (upper Darriwilian, Middle Ordovician). The genera *Drepanodus*, *Drepanoistodus*, *Gothodus*, *Panderodus*, *Periodon, Protopanderodus, Sagittodontus* and *Triangulodus* and are also represented.

The Darriwilian conodont assemblages from Bellewstown and Tramore in Ireland are characteristic of the 'eastern' Iapetus Ocean with a southern mid latitudinal position. The fauna resembles the San Rafael (Mendoza Province, Argentina) conodont fauna of the Cuyania Composite Terrane. *Baltoniodus*, *Eoplacognathus* and *Sagittodontina* are shared with faunas in Baltica, whereas *Baltoniodus* and *Sagittodontina* together with *Yangtzeplacognathu*s occur in South China and *Plectodina* and *Yangtzeplacognathus* are recorded from Gondwana. An important factor influencing the distribution of conodont taxa is the siliciclastic-dominated sedimentation, interpreted to reflect cool to temperate water conditions. The Bellewstown and Tramore conodont fauna is in marked contrast to other deposits on island arcs and back-arc terranes within the Iapetus. These are interpreted to represent low latitudinal, warmer, oceanic water conditions with Laurentian faunal affinity. Some potential new species are introduced in open nomenclature.

Keywords. – Conodonts, Bellewstown Terrane, Leinster-Lakesman Terrane, Bellewstown Limestone Member and Tramore Limestone Formation, Ireland, late Middle Ordovician.

Introduction

In east and southeast Ireland Ordovician marine sedimentary rocks yielding late Darriwilian (Dw3; Llanvirn, Middle Ordovician) conodonts are known from the Bellewstown Terrane and the Tramore Limestone Formation of the Leinster–Lakesman Terrane (Fig. 1; Bergström and Orchard 1985; Harper and Parkes 2000). Most previous studies on Ordovician conodonts from eastern and southern Ireland have been of a preliminary character with focus on the biostratigraphical implication of the fauna. It comprises a list of conodont species (Brenchley *et al*. 1977), brief reports (Bergström and Orchard 1985, specifically contribution by George Sevastopulo on p. 44–6), with further information in Bergström (1971) and Bergström *et al*. (1974). Subsequent, more complete studies of Ordovician conodonts from Ireland are those of the Upper Ordovician (Katian) Portrane Limestone Formation in eastern Ireland (Ferretti *et al*. 2014), and the Early Ordovician fauna recovered from limestone blocks in the Rosroe Formation of the South Mayo Trough, western Ireland (Stouge *et al*. 2016a). The latter fauna is comparable to the Tourmakeady Limestone and both are of Laurentian affinity.

The known stratigraphic record from eastern and southeastern Ireland (summarised in Molyneux *et al*. 2023 and references therein) covers most of the period, but information based on new material and the description and revision of older collections from this study are critical for a better understanding of the east and southeast parts of Ireland that originally faced the Iapetus Ocean. The closest contemporaneous, but mostly younger strata are located in Wales, now separated by the Irish Sea, but situated on the Avalonia Terrane in the Ordovician (Cocks and Torsvik 2002, 2005, 2006, 2021; Cocks and Fortey 2009; Landing *et al*. 2020, 2022).

This paper describes the late Darriwilian (Llanvirn; Middle Ordovician) conodonts recovered from both the Bellewstown Limestone Member (of the Carnes Formation) and the Tramore Limestone Formation (of the Duncannon Group). It will place the faunas in a currently accepted stratigraphic context and briefly discuss their palaeoecologic–palaeobiogeographic significance.

Geological setting

The Ordovician geology of east and southeast Ireland falls into a series of lithologically distinct and fault zone-, mylonite- and lineament-bounded terranes and sub-terranes (McConnell 2000; McConnell *et al*. 1991, 2010, 2021; Murphy *et al*. 1991; Todd *et al*. 1991; Harper and Parkes 2000; van Staal *et al*. 2021; Molyneux *et al*. 2023, fig. 1 therein). The conodonts from the two locations dealt with here derive respectively from the Bellewstown Terrane adjacent to the Iapetus suture and the Leinster-Lakesman peri-Gondwanan Terrane with an origin on the margins of the Gondwana continent and with a position to the south of the Iapetus Suture (Fig. 1).

The Bellewstown Terrane is composed of volcanic rocks, along with contemporaneous volcaniclastic and siliciclastic sedimentary rocks with minor interbedded limestones. It is derived from an arc setting and lies adjacent to the Leinster-Lakesman Terrane. The latter terrane is composed of Ordovician sedimentary rocks lacking exposures of basement and Cambrian rocks. The Leinster-Lakesman Terrane has been compared with the Ganderia Terrane in the Appalachians (van Staal *et al*. 2021; McConnell *et al*. 2021).

Investigated localities

The Ordovician conodonts investigated in this report were recovered from calcareous sandstone and silty limestone samples collected from outcrops exposed respectively at Bellewstown and Tramore (Fig 1).

Bellewstown

Sedimentary rocks assigned to the Bellewstown Terrane occur in the northern part of the Balbriggan inlier, County Meath, eastern Ireland. The Slane Fault separates the terrane from the Grangegeeth Terrane and the Central Terrane and the southern boundary with the Leinster-Lakesman Terrane is the Lowther Lodge Fault. The Bellewstown Terrane rifted from Gondwana and occupied a position in the eastern Iapetus Ocean (van Staal *et al*. 2021; Molyneux *et al*. 2023). According to McConnell *et al*. (2015, 2021) the main volcanism of the Bellewstown Subterrane occurred at c.474Ma (i.e. Floian, Early Ordovician).

Stratigraphy. The Lower Ordovician Prioryland Formation consists of fine siliciclastic sedimentary rocks with interbedded slump breccias. The overlying volcanogenic rocks, associated with siltstones, sandstones and volcanogenic breccias are assigned to the Hilltown Formation (Llanvirn; Darriwilian, mid Ordovician). The Hilltown strata are conformably to disconformably overlain by the Carnes Formation, which contains the Bellewstown Limestone Member at its base. This member is composed of calcareous sandstone and sandy or impure limestone with some volcaniclastic units (Harper and Rast 1964). The succession of the Carnes Formation and above the Bellewstown Limestone Member is unnamed. It consists of c.300m of greywacke, shale and mudstone (Llandeilo to Caradoc; Darriwilian into Sandbian; McConnell *et al*. 2015). The strata of the Bellewstown

Limestone Member were deposited under deepening conditions starting in the late Darriwilian and extending into the early Sandbian.

Fauna and biostratigraphy. Harper and Rast (1964) recorded Darriwilian (Llanvirn) shelly fossils from the Bellewstown Limestone Member. Shelly fossils from the Prioryland Formation and the Bellewstown Limestone Member (of the Carnes Formation) are assigned to the Celtic Province (Harper and Parkes 1989; Harper *et al*. 1990, 2013; Harper 2023); the fauna of the Carnes Formation (above the level of the Bellewstown Limestone Member) has an Anglo-Welsh character (Brenchley *et al*. 1977; Harper *et al*. 1990; Molyneux et *al*. 2023; Harper 2023).

Brenchley *et al*. (1977) listed Darriwilian (Llanvirn) and Sandbian (Caradoc) conodonts from the Bellewstown Limestone Member. Bergström and Orchard (1985) reported the conodont species *Eoplacognathus robustus* Bergström, 1971 from the same unit. Float limestone boulders in the beach west of Bellewstown yielded additional conodonts (Bergström and Orchard 1985, pl. 2.2, figs 8, 12), which are assigned to the *Pygodus serra* Zone. The upper part of the Carnes Formation yielded graptolites referred to the *Nemagraptus gracilis* Zone (Caradoc; Sandbian, Upper Ordovician).

Tramore

The Tramore Limestone Formation in southeastern Ireland is exposed in the sea cliffs extending along the coast between the Tramore Bay in the east and Ballydowane Bay in the west (Fig. 1; Carlisle 1979; Wyse Jackson *et al*. 2001; Liljeroth *et al*. 2017).

Stratigraphy. The Tramore Limestone Formation is c.49m thick at Tramore strand, but reaches a maximum of 65m. The stratotype section is at Barrel Strand (see Liljeroth *et al*. 2017, fig. 4). The unit is predominantly composed of siliciclastic sedimentary rocks, often calcareous, with interbeds of silty limestone beds and nodular limestone horizons in the middle of the formation. It is assigned to the Duncannon Group, which also includes the deeper to deep-water Dunabrattin Limestone Formation, which is predominantly composed of sandstone, siltstone and shale with minor limestone (over 500m thick). The Tramore Limestone Formation represents shallow-water deposition on the shelf, whereas the Dunabrattin Limestone was a coeval, deeper to deep-water slope equivalent (Carlisle 1979; Harper and Parkes 2000; Key *et al*. 2005; Liljeroth *et al*. 2017). Both formations were deposited under deepening conditions during the late Darriwilian and early Sandbian.

Carlisle (1979) subdivided the Tramore Limestone Formation into six informal lithological units. Unit 1 is a c.2m thick basal conglomerate/breccia. The overlying unit 2 consists of c.12m of bedded calcareous sandstone and impure limestone. Above this, unit 3 consists of siltstones with minor interbeds of limestone. The higher units 4, 5 and 6 are largely composed of shale and siltstone with some nodular limestone and minor beds of impure limestone.

Fauna and biostratigraphy. Biostratigraphically, the Tramore Limestone Formation ranges from upper Darriwilian (Dw3; Llanvirn; Harper and Rast 1964) extending into the lower Sandbian (Sa1; Llandeilo–Caradoc, Upper Ordovician). The shelly fossils from the formation include bryozoans, brachiopods, cephalopods, corals, echinoderms, gastropods and trilobites (Wyse Jackson *et al*. 2001, and references therein); graptolites have been recorded from black shales (Baily 1865). The brachiopod fauna is of mixed faunal affinity changing upsection from the Celtic Province to an Anglo-Welsh fauna (Parkes and Harper 1996; Liljeroth *et al*. 2017; Harper 2023).

Brenchley *et al*. (1977) listed conodonts from the Tramore Limestone Formation that are largely late Darriwilian (late Middle Ordovician) with a range into the lower Sandbian (early Late Ordovician). Bergström (1971) and Bergström and Orchard (1985) reported the presence of *E. lindstroemi* (Hamar, 1964) from the formation (late Darriwilian), but did not provide information on a specific horizon in the section.

Harper and Parkes (2000) and Liljeroth *et al*. (2017, fig. 4) assigned units 1 and 2 to the *Hustedograptus teretiusculus* Graptolite Zone and higher units of the formation are assigned to the *Nemagraptus gracilis* Graptolite Zone. The precise position of the base of Upper Ordovician in the section, however, is not precisely known, but was tentatively placed at the base of unit 3 by Liljeroth *et al*. (2017).

Material and methods

The investigated microfossil material consists of a series of microslides containing conodonts from the collections of the late George Sevastopulo, who passed over the material to the authors for further inspection. The major part of the investigated microslides are from the Bellewstown locality (Tables 1–3) and a moderate number of slides are from the section at Tramore (Table 4).

The investigated material from the Bellewstown area was collected from two exposures in the northern part of the Balbriggan inlier (Bergström and Orchard 1985, p. 46). Additional samples include float limestone boulders from Bellewstown beach (Bergström and Orchard 1985, p. 46; own collection). The Bellewstown microslides are labelled BellWest 1–6, 8–16 and BellEast 1–7. Additional microslides were respectively labelled BellN samples I to V, B and C. One additional sample, Bellewstown #75 (BellN 75), was collected from a limestone boulder at the beach next to the cliff (Table 3; own collection). Additional information on collected horizons of the samples in the succession, along with processed sample size, is not available. The 30 conodont-bearing microslides from Bellewstown provide a total of 2985 identifiable conodont elements, which have all been inspected (Tables 1–3).

The Tramore Limestone Formation collection comprises a continuous series of 14 microslides, labelled no. 1 to 15 (slides 7 and 11 are missing) with a total of 220 conodont elements. Four of these slides were barren of conodonts but contain ‘steinkerns’ of gastropods and ostracods. Although the stratigraphic position of the individual samples collected from the succession is not well established, some information, written on the microslides such as ‘base of limestone’ and ‘c.14m above base’, indicate that the collected samples were derived from the lower Tramore Limestone Formation (units 1 and 2, perhaps extending into lower unit 3).

The highest yield from the entire sample set was produced by the Bellewstown East samples, the Bellewstown West and North float samples and also the higher collection numbers at Tramore (Tables 1–4). The preservation of the conodont specimens varies from fragmented, as the specimens are fragile, to relatively well-preserved specimens. Sedimentary grains still adhere to many conodont elements and it was not possible to remove this material without damaging specimens. The grains have in some cases obscured the diagnostic characters hindering specific determination. Many of the specimens show a cleavage cutting individual elements, but they are not all broken due to a secondary recrystallisation that has re-cemented them together. Despite such secondary effects many specimens preserve their original delicate surface structures such as striae and polygonal patterns.

The majority of the conodont elements are black in colour (i.e. the Conodont Alteration Index (CAI) equals 5; Epstein *et al*. 1977; Bergström 1980). Some specimens, however, are light brown to nearly translucent, which is CAI 6 to 6.5 (Rejebian *et al*. 1987). Accordingly, and as a minimum, the Ordovician host rocks have been heated to 360 ºC.

Visual and statistical analysis of conodont elements

All microfossil samples (a total of 3205 conodont elements, plus many fragments), have been sorted, identified and investigated. The illustrated specimens (Figs 2–5) were photographed using a Tescan Mira SEM of the Department of Geosciences and Natural Resource Management (IGN) at the University of Copenhagen, Denmark. Multivariate analysis of the conodont fauna was conducted using PAUP statistical software (Hammer 2023; Hammer *et al*. 2001; Hammer and Harper 2024). Very rare taxa and very low yielding samples were excluded from the biofacies analysis. The Morisita similarity coefficient was applied for the normal cluster biofacies analysis (Q and R mode); the correlation similarity coefficient has been applied for the PC analysis. However, other similarity coefficients were tested here and provided largely similar results.

Repository

Figured specimens and assemblage slides are housed in the Trinity College Dublin Geological Museum, Ireland, catalogue numbers TCD.65058–65160.

Taxonomic notes

Several conodont taxa illustrated here occur in low to very low numbers and do not provide any significant new information. These are listed here with short comments; the total number of conodont specimens is provided in Tables 1 to 4.

Genus ANSELLA Fåhræus and Hunter, 1985a

Type species. *Belodella jemtlandica* Löfgren, 1978.

Ansella sp.

Fig. 2.1–2.2

Remarks. The specimens, here assigned to the genus *Ansella*, are compressed, biconvex to planoconvex and keeled. The basal cavity is deep with a tip situated close to the anterior margin of the base. Additional specimens typical of the *Ansella* apparatus have not been recorded. The specimens are from Bellewstown East, sample BellEast 1 and Tramore, sample Tram 14.

Genus DREPANODUS Pander, 1856

Type species. *Drepanodus arcuatus* Pander, 1856.

Drepanodus sp.

Fig. 2.3–2.4

Remarks. The specimens, mainly arcuatodontiform elements, are assigned to the genus *Drepanodus* Pander, 1856 *sensu* Löfgren and Tolmacheva (2003). *Drepanodus* sp. is closely similar to the specimens named *Drepanodus* sp. and figured by Bergström and Ferretti (2018, fig. 6w). The specimens are recorded in low numbers from Bellewstown East (Table 1), Bellewstown West (Table 2) and Tramore (Table 4).

Genus PERIODON Hadding, 1913

Type species. Periodon aculeatus Hadding, 1913.

Periodon aculeatus Hadding, 1913

Fig. 3.13–3.17

Remarks. All recorded *Periodon* elements are assigned to *P. aculeatus* Hadding, 1913. This species was recovered from the Bellewstown Limestone Member and Tramore Limestone Formation but in low numbers in both units.

Genus PHRAGMODUS Branson & Mehl, 1933

Type species. *Phragmodus primus* Branson and Mehl, 1933.

Remarks. The concept of the genus *Phragmodus* follows that of Dzik (1978) and Leslie and Bergström (1995); the latter authors recognised that seven elements comprise the apparatus.

Phragmodus polonicus Dzik, 1978

Fig. 5.9–5.12

Remarks. In the Bellewstown and Tramore material the pastinate pectiniform elements are represented by two forms that are distinguished by the angle between their lateral and adenticulate anterior process. Pa element processes enclose a 10–20º angle, whereas those of Pb element enclose a 70–80º angle. The possible geniculate coniform M element is adenticulate; a quadriramate S element may represent the Sd element.

The M element of *Phragmodus polonicus* is geniculate coniform, which is similar to *P. undatus* Branson and Mehl, 1933. Consequently, *P. polonicus* and *P. undatus* are probably closely related. ?*Phragmodus flexuosus* of Ethington and Clark, 1982 has a geniculate adenticulate coniform element similar to the Irish specimen. Although these authors did not record two pectiniform elements, it is possible that ?*Phragmodus flexuosus sensu* Ethington and Clark represents the same or at least a closely related species.

The M elements of *P. flexuosus* Moskalenko, 1973 and *P. inflexus* (Stauffer, 1935a) are distinguished from *P. polonicus* and *P. undatus* mainly by the presence of denticles on the upper margin of the base of the element (= cyrtoniodontiform; cf. Sweet 1981a; Leslie and Bergström 1995). In the material from Ireland, *Phragmodus polonicus* is rare and the specimens are small; the taxon is recorded sporadically from the Tramore Limestone Formation and also from the Bellewstown Limestone Member at Bellewstown East.

Genus PROTOPANDERODUS Lindström, 1971

Type species. *Acontiodus rectus* Lindström, 1954.

Protopanderodus varicostatus (Sweet and Bergström, 1962)

Fig. 2.6–2.7

Remarks. The specimens resemble those illustrated by Mellgren *et al*. (2012, fig. 5W, X) and assigned to *P. calceatus* Bagnoli and Stouge, 1997. *Protopanderodus varicostatus* is rare in the collection and is recorded from Bellewstown East and Tramore.

Genus PSEUDOONEOTODUS Drygant, 1974.

Type species. *Oneotodus*? *beckmanni* Bischoff and Sannemann, 1958.

Pseudooneotodus mitratus (Moskalenko, 1973)

Fig. 2.5

Remark. The single specimen has been recorded from sample BellWest 1 at Bellewstown West.

Genus PYGODUS Lamond and Lindström, 1957

Type species. *Pygodus anserinus* Lamont and Lindstrom, 1957.

Remarks. The *Pygodus* apparatus is here considered to be septimembrate and composed of pygodontiform (Pa), haddingodontiform (Pb), ramiforms (Sa–Sd) and geniculate (M) elements.

Pygodus serra (Hadding, 1913)

Fig. 3.18–3.19

Remarks. The material comprises Pb (haddingodiform) and M elements. The latter is a falodontiform that here is tentatively assigned to *Pygodus serra* (Hadding, 1913). The M element at hand is denticulate on the anterior edge of the anterior process. The cusp is curved with the tip pointing towards the anterior when observed in lateral view. The M element is similar to the 'ne element' of Dzik (1994, text-fig. 27) and the M element that Paiste *et al*. (2022, fig. 7H) tentatively assigned to the *P. anserinus* apparatus. The *Pygodus* specimens are recorded from Bellewstown Limestone Member at Bellewstown West, Bellewstown A and from sample Tram 14 of the Tramore Limestone Formation.

Genus TRIANGULODUS van Wamel, 1974

Type species. *Paltodus volchovensis* Sergeeva, 1963.

Triangulodus alatus Dzik, 1976

Fig. 2.18

Remarks. The specimens conform well to the species diagnosis. The taxon is rare, but is recorded from the Tramore Limestone Formation sample Tram 14 (14m above base of formation) and from Bellewstown East, Bellewstown West and Bellewstown A.

Genus et sp. indet. A

Fig. 2.20–2.24

cf. 1984 *Acodus*? n. sp. Stouge, p. 76–7, pl. 14, figs 20–28

Remarks. Genus indet. sp. A is composed by a series of reclined, keeled and costate simple cones and a geniculate element. The cusp is tall, wide and laterally compressed; the base is small. Some specimens may have one or are serrated distally on the anterior short process.

The apparatus of Genus et sp. indet sp. A is incompletely preserved, but P, M, and Sd elements are recorded. *Acodus*? sp. Stouge, 1984 shares similarities with the specimens and the two taxa may represent the same genus. The specimens of Genus et sp. indet A are recorded from Bellewstown East, Bellewstown West, Bellewstown A and sample Tram 14 at Tramore.

Genus et sp. indet. B

Fig. 2.19

2023 *Semiacontiodus* sp. cf. *S. davidi* Löfgren, 1969; Albanesi *et al.*, fig. 9R–T

Remarks. Genus et sp. indet. B comprises simple suberect to recurved cones with a small base. The elements are rounded in cross-section and with a striated surface. Albanesi *et al*. (2023) illustrated similar specimens from the Santa Gertrudis Formation of the Cordillera Oriental, in northwest Argentina. However, other than this taxon, the Argentinian conodont fauna is completely different to the Irish conodont assemblage. The presence of Genus et sp. indet. B is erratic and with low abundance in the collection, but it is recorded from Bellewstown East, Bellewstown A and in samples from the Tramore section.

Genus et sp. indet C

Fig. 2.16–2.17

2022 ?*Baltoniodus* sp. Ferretti and Bergström, fig. 8X–Y

Remarks. Adentate Sc and Sd elements with a curved and keeled cusp; the base is triangular with an arched upper margin. The Sc element is moderately bent laterally. The Sd element has an outer and an inner costa; both extend from the tip of the cusp to the aboral margin of the base. Additional elements that could be assigned to the apparatus were not identified. The specimens are recorded from Bellewstown West.

Systematic palaeontology

The more abundant and best-preserved conodont specimens are described in this section. The synonymies presented are relatively short, as the taxa have been described previously. The synonymy list includes reference to papers where extensive description and detailed information are documented, necessary for complete understanding of the taxa. Some potential new taxa are detailed but introduced informally.

The descriptions use the elements shape category terminology P-M-S as shortage for many of the elements (e.g. Sweet and Schönlaub 1975; Clark *et al*. 1981; modified by Cooper 1975; elaborated further by Sweet 1988b). The P-M-S annotations do not relate to anatomical 'position' in a natural skeletal apparatus, as the apparatus is unknown for the taxa described here (see discussion in Aldridge and Purnell 1996; and recommendations by Purnell *et al*. 2000). The elements of simple cone taxa such as *Drepanoistodus* and *Drepanodus* are assigned to the 'form element' genera with the addition –'idontiform'.

Phylum CONODONTA Pander, 1856

Genus BALTONIODUS Lindström, 1971

Holotype. *Prioniodus navis* Lindström, 1971.

Baltoniodus alatus (Hadding, 1913)

Fig. 3.1–3.8

non 1879 *Prioniodus*? *alatus* Hinde, p. 361, pl. XVI, fig. 5

1913 *Prioniodus alatus* n. sp. Hadding, p. 32, pl. 1, figs 9–10

1955 *Prioniodus alatus* Hadding; Lindström, p. 113, pl. 22, figs 26, 28–34 cf. 1966 *Prioniodus alatus* Hadding; Fåhræus, pp 28–9, pl. IV, fig. 4a–c (= Pa element *B. prevariabilis* Fåhræus, 1966)

1971 *Prioniodus prevariabilis* Fåhræus; Bergström, pp 146–7 (*cum syn*.), pl. 2, fig. 1

1976 *Prioniodus alatus alatus* Hadding; Dzik, pp 436–7 (*cum syn*.), text-fig. 24a–g

1981 *Prioniodus prevariabilis* Fåhræus; Nowlan, p. 12, pl. 2, figs 6, 11, 12, 13

1998c *Baltoniodus prevariabilis* (Fåhræus); Zhang, p. 54 (*pars*), pl. 3, figs 1–8

pars 1994 *Baltoniodus prevariabilis* (Fåhræus, 1966); Dzik, pp 82, 84, pl. 18, figs 17–22, text-fig. 14b

1999a *Baltoniodus prevariabilis* (Fåhræus 1966); Lehnert *et al.*, p. 37, pl. 1, figs 2, 3, 8–14

1999b *Baltoniodus prevariabilis* (Fåhræus 1966); Lehnert and Bergström, pl. 1, fig. 15

2001 *Baltoniodus prevariabilis* (Fåhræus, 1966); Rasmussen, pp 57–8 (*cum syn*.), pl. 3. figs 1–3

2011 *Baltoniodus prevariabilis*; Viira, fig, 6D–F, H, K, M, Q–S

2012 *Baltoniodus prevariabilis* (Fåhræus); Hints *et al.*, fig. 5J–K

pars 2015 *Eoplacognathus robustus* Bergström; Heredia and Mestre, pl 1, fig. 14 only

2016b *Baltoniodus prevariabilis* (Fåhræus); Stouge *et al.*, fig. 3A–B

2016 *Baltoniodus prevariabilis* (Fåhræus); Wu *et al.*, fig. 3:1

2019 *Baltoniodus prevariabilis* (Bergström); Heredia and Mestre, p. 563, fig. 5G–M

pars 2019a *Eoplacognathus robustus* Bergström; Heredia and Mestre, fig. 3J (only, M element)

pars 2019b *Eoplacognathus lindstroemi* Bergström; Heredia and Mestre, fig. 4E (only, M element)

2019b *Baltoniodus prevariabilis* (Fåhræus); Heredia and Mestre, fig. 6

2022 *Baltoniodus prevariabilis* (Fåhræus, 1966); Ferretti and Bergström, fig. 8M–U, Z–B′, fig. 9O, 9P

2022 *Baltoniodus prevariabilis* – Paiste *et al.*, fig. 5A–R

Type locality and horizon. Locality E15, Fågelsång, Scania, Sweden.

Material. 273 elements (Pa 71, Pb 74, M 38, Sa 13, Sb 20, Sc 21, Sd 36).

Remarks. Hadding (1913) assigned specimens of *Baltoniodus alatus* (Hadding, 1913) to the form element genus *Prioniodus* Pander, 1856. Bergström (1971, 2007a) synonymised the species with *Prioniodus prevariabilis* (Fåhræus, 1966), an approach which has been followed by many authors. Dzik (1976), however, reintroduced the species *Prioniodus alatus* Hadding, and later (Dzik 1994) assigned the species to the multielement genus *Baltoniodus* Lindström, 1971 but synonymised the species with *B. prevariabilis*.

The specimens from Ireland are identical to the form species *Prioniodus alatus* Hadding, 1913. Lindström (1955) described in detail the Pa element of *B. alatus* Hadding, which is the type specimen of the species. A well-developed and visibly inwardly flexed basal margin is developed along the basal margin of the processes on the elements. In upper view the basal sheath of the posterior process is expanded and developed as a prominent inner flare, especially on larger to large specimens of the Pa element; on small or smaller specimens this flare is omnipresent but less prominent. Some large specimens inspected here are distorted (i.e. Fig. 3.2), however their overall aspect is similar to that of *Baltoniodus alatus* (Hadding, 1913).

Baltoniodus alatus represents the evolutionary stage between the older *B. prevariabilis* (Fåhræus, 1966) and its successor *B. variabilis* (Bergström, 1971). It differs from *B. prevariabilis* in the development of the prominent inner flare of the base on the Pa element and the basal sheath is lower. In *B. variabilis* the margin along the aboral margin on the Pa element is developed to become a narrow platform on the processes and has a sharp edge along the basal margin of the base (seen in large specimens; cf. Bergström 1971; Dzik 1994).

The multielement genus *Baltoniodus* Lindström, 1971 is not related to the Devonian multielement taxon, which includes the form element species *Prioniodus*? *alatus* Hinde, 1879 (Hinde 1879, p. 361, pl. XVI, fig. 5) and *Baltoniodus alatus* (Hadding) is considered a valid name for the multielement species recorded here.

In their reconstruction of the genus *Eoplacognathus* Heredia and Mestre (2019) added M elements to the apparatus that indeed resemble those of *B. alatus*; consequently, these are placed in into synonymy here.

Occurrence. Several samples from Bellewstown East, West and N (Tables 1-3) and from Samples Tram 10 and Tram 14 at Tramore (Table 4).

Distribution. *Baltoniodus alatus* was first recorded from locality E15, Fågelsång, Scania, Sweden. It occurs widely across the Baltic palaeobasin, usually 'hidden' under the name *Baltoniodus prevariabilis*. It is common in the Flags and Grits Formation, Fairfach, and the Llandeilo Limestone, South Wales, UK. The species ranges from the *E. reclinatus* Conodont Subzone into the lower *Pygodus anserinus* Conodont Zone (top Darriwilian – lower upper Sandbian, Middle Ordovician; top Llanvirn).

Genus BELODELLA Ethington, 1959

Type species. *Belodus devonicus* Stauffer, 1940.

Remarks. Belodella has an apparatus composed of slender, deeply excavated, keeled coniform elements with a denticulate and distally keeled upper margin of the base.

Belodella serrata Dzik, 1976

Fig. 5.1–5.4

1976 *Belodella serrata* sp. n. Dzik, p. 422, text-fig. 14f, pl. XLI, fig. 3

1981 *Panderodus* aff. *P. serratus* Rexroad; Nowlan, p. 12, pl. 1, figs 16, 18

non 2012 *Ansella serrata*; Hints *et al.*, fig. 6N, Q

2022 *Panderodus alabamensis* (Sweet and Bergström, 1962); Ferretti and Bergström, p. 481 (*pars*), fig. 10A–D

Type section and horizon. Erratic boulder E-141, Miedzyzdroje, northwest Poland.

Material. 73 specimens.

Description. The rostrate specimens are long with a relatively high base tapering towards the tip of the cusp. Elements are laterally compressed with upright to antero-inclined small and basally fused denticles extending from the middle of the upper margin of base continuing onto the lowermost part of the of the cusp in some specimens. The cusp is relatively short and varies from recurved, suberect to inclined towards the anterior. The base varies from low to higher and from short to longer with a deeply excavated basal cavity with a tip that continues into the cusp.

A prominent upper keel is high, short and well-developed on the distalmost posterior part of the upper margin of the base on the specimens with long bases. The specimens vary from convex, planoconvex to concave-convex in cross section. The elements range from straight in one plane, slightly to strongly bent laterally towards the plano- and concave side.

Remarks. *Panderodus* aff. *P. serratus* Rexroad *sensu* Nowlan (1981) probably belongs here. Some authors (e.g. Mellgren 2010; Ferretti and Bergström 2022) assigned *Belodella serrata*-like specimens to the multielement genus *Panderodus*. Others assign similar denticulate elements to the multielement genus *Ansella* (i.e. Hints *et al*. 2012). Here, *Belodella* is characterised by elements with a characteristic keel (or heel) distally on the upper margin of the base and with elements forming a lateral bend. Such features are not typical or common for *Panderodus* elements.

The material to hand did not provide any trace of a geniculate element typical of *Ansella* that could be associated with the denticulate specimens. At this stage the specimens are assigned to the species *Belodella serrata* Dzik, 1976.

Occurrence. *Belodella serrata* is well represented and common in samples from the Bellewstown collections, eastern Ireland.

Distribution. The species is recorded from Holy Cross Mountains, Poland (Dzik 1976, 1994), Baltoscandia, central New Brunswick, Canada and southern Ireland (upper Darriwilian; upper Llanvirn–Llandeilo; Middle Ordovician).

Genus DREPANOISTODUS Lindström, 1971

Type species. *Oistodus forceps* Lindström, 1954.

Drepanoistodus sp. A

Fig. 2.8–2.10

1999 *Drepanoistodus suberectus* (Branson and Mehl, 1933); Lehnert *et al.*, p. 39, pl. 2, fig. 2

2012 *Drepanoistodus* cf. *suberectus* (Branson and Mehl, 1933); Mellgren *et al*, fig. 5AH, AI

2018 *Drepanoistodus suberectus* (Branson and Mehl, 1933); Bergström and Ferretti, fig. 6t–v

2018 *Drepanoistodus* sp. Heward *et al.*, p. 76, fig. 10i–k (only)

2018 *Drepanoistodus* sp. Lindström, 1971; Miller *et al.*, pp 583, 585, fig. 8A–I, ?E, ?H

2022 *Drepanoistodus suberectus* (Branson and Mehl, 1933); Ferretti and Bergström (*pars*), fig. 12B, C–F (only)

Material. 149 specimens (84 drepanodiforms, 25 suberectid and 40 oistodontiforms).

Diagnosis. Oistodontiforms with a short and nearly quadratic base in lateral view. All elements are keeled and with smooth outer fae of the cusp and an inner carina. Cross section of cusp varies from biconvex, rounded to plano-convex on all elements.

Description. The oistodontiform elements have a small and nearly quadratic base in lateral view. Their cusp is reclined, and the posterior margin of the cusp forms an angle with the upper basal margin at c.30°. The cross section of the cusp is sub-circular to convex. An inner broad carina may be developed on the cusp. The upper margin of the base is short and keeled. The basal cavity is open and wide. The cusp of drepanodontiform elements is sub-circular, convex to planoconvex in cross section and the antero-basal corner may be pointed.

Remarks. The keeled elements characteristically are relatively rounded, rather than compressed. The small quadratic base of the oistodontiform elements is diagnostic. The drepanodiform elements of *Drepanoistodus suberectus sensu* Bergström and Ferretti (*pars*) are likely drepanodiform elements of the same species. Also, *Drepanoistodus* sp. of Miller *et al*. (2018) and Heward *et al*. (2023 with references) appears similar to the Irish material and is added to the synonymy list.

Drepanoistodus sp. A is a new species that is characteristic of shallow-water deposits; here it is introduced informally since its stratigraphic horizon is unknown.

Occurrence. This species is present to common in most samples from both the Bellewstown Limestone Member and lower part of the Tramore Limestone Formation (Tables 1–4).

Distribution. *Drepanoistodus* sp. A is also recorded from olistoliths in debris flows of the Garn Formation, Anglesey, north Wales. It is recorded from the sultanate of Oman and perhaps also from Saudi Arabia. It is common in Baltoscandia.

Drepanoistodus sp. B

Fig. 2.11–2.15

1999a *Drepanoistodus basiovalis* (Sergeeva, 1963); Lehnert *et al.*, pp 37–8, pl. 2, fig. 10

1999a *Drepanoistodus suberectus* (Branson and Mehl, 1933); Lehnert *et al.*, p. 39, pl. 2, fig. 9 (only)

1999b *Drepanoistodus venustus* (Stauffer 1935); Lehnert and Bergström *in* Lehnert *et al.* 1999b, pl. 2, fig. 5

2016 *Drepanoistodus* sp. Heward, fig. 10h–k

2018 *Drepanoistodus suberectus* (Branson and Mehl, 1933); Bergström and Ferretti, fig. 6t-u

2018 *Venoistodus venustus* (Stauffer, 1935); Bergström and Ferretti, fig. 6x

2022 *Drepanoistodus suberectus* (Branson and Mehl, 1933); Ferretti and Bergström (*pars*), fig. 10I, fig. 12A, G–I

Material. 135 specimens (90 drepanodontiforms, 14 suberectid and 31 oistodontiforms).

Diagnosis. Oistodontiform element with reclined cusp, semi-long keeled base, a pointed postero-basal corner and prominent inner carina on cusp. The antero-basal corner of the drepanodiforms may be pointed and extended downwards.

Description. The oistodiform element is with a reclined cusp and semi-long base. The posterobasal corner meets the upper margin of the base with the basal margin in an acute to rectangular angle given a pointed to rounded aspect. The keeled upper margin of the base continues on to cusp and up to the tip. A prominent inner, median carina is present on the cusp. The drepanodiform elements are laterally compressed with a flat convex to plano-convex aspect in cross-section.

Remarks. The lateral compressed drepanodiform elements are relatively more 'elegant' in appearance when compared the rounded elements of *Drepanoistodus* sp. A. The pointed and short extension of the anterobasal corner of the base is characteristic for some of the drepanodiform elements of this species. The specimens appear in samples that represent relatively offshore to distal deposition on the shelf.

Occurrence. The species is present in the samples from Bellewstown Limestone Member and upper parts of the lower Tramore Limestone Formation (see Tables 1–4).

Distribution. This taxon is recorded from the Garn Formation, Anglesey, north Wales. It is also recorded from the Peletay Member of the Lindero Formation, San Rafael Block, Mendoza Province, Argentina. *Drepanoistodus* sp. B is common on Baltscandian platform.

Genus EOPLACOGNATHUS Hamar, 1966

Holotype. *Ambalodus lindstroemi Hamar*, 1966.

1998b *Baltoplacognathus* Zhang, p. 24

Remarks. The multielement genus *Eoplacognathus* Hamar, 1966 comprises paired platform (Pa and Pb) elements. The Pa elements have four or five branches (= polygnathodontiform) and Pb (= ambalodondiform) elements are with three Y- and T-shaped branches. The paired elements are developed with distinct morphologies and left (sinistral) and right (dextral) elements are not identical or mirror images of each other (e.g. Bergström 1971; Viira 1972; Zhang 1998b; Stouge and Bagnoli 1999). In upper view the Pa elements may vary from lateral bent to straight elements.

The Bellewstown and Tramore samples yield well-represented specimens of the genus *Eoplacognathus* Hamar. Zhang (1998b) erected the genus *Baltoplacognathus* and considered it to form an evolutionary lineage composed of the species *B. reclinatus* and *B. robustus*. However, these two *Eoplacognathus* species evolved via *E. lindstroemi* into *E. elongatus*, which is the ultimate species of the *Eoplacognathus* lineage (in accordance with Bergström 1971, 1983; Stouge and Bagnoli 1999). Accordingly, the species recorded here are assigned to the genus *Eoplacognathus*.

Here, *Eoplacognathus reclinatus* extends into the lower *E. robustus* Conodont Subzone of the *Pygodus serra* Conodont Zone. A third group occurring together with *E. reclinatus* and *E. robustus* is referred to cf. *E. robustus* Bergström, 1971.

Eoplacognathus reclinatus (Fåhræus, 1966)

Fig. 4.16–4.23

1966 *Ambalodus reclinatus* n. sp. Fåhræus, pp 19–20, pl. IV, fig. 3a, b (holotype)

1971 *Eoplacognathus reclinatus* Fåhræus n. sp.; Bergström, pp 139–40 (*cum syn*.), pl. 1, figs 11–13

1974 *Eoplacognathus reclinatus* (Fåhræus, 1966); Viira, pp 81–2, pl. VIII, figs 12–13, 93, 94

1974 *Polyplacognathus ramus* n. sp.; Viira, pp 110–11, 138, text-fig. 140

1976 *Eoplacognathus lindstroemi reclinatus* (Fåhræus); Dzik, p. 433, fig. 31g–k

1998c *Baltoplacognathus reclinatus*; Zhang, pp 10–11, figs 7A–G, 11B1

1999a *Eoplacognathus foliaceus* Fåhræus; Lehnert *et al*., p. 39, pl. 2, fig. 1, 3, 6, 8, 12–(?13), 14

1999b *Eoplacognathus reclinatus* (Fåhræus 1966); Lehnert and Bergström *in* Lehnert *et al.*, pl. 1, figs 10, 13, 14, 17

2011 *Yangtzeplacognathus foliaceous* (Fåhræus); Viira, p. 7, fig. 5N–O

2012 *Baltoplacognathus reclinatus* (Fåhræus); Hints *et al.*, p. 216, fig. 5A, B, ?C

2012 *Eoplacognathus foliaceous* (Fåhræus, 1966); Mellgren *et al.* (*pars*), fig. 6J, Q, 6C?, not 6A (= *Lenodus pseudoplanus* late form)

2016b *Baltoplacognathus reclinatus* (Fåhræus); Stouge *et al.*, fig. 3C–D

Type section and type horizon. Güllhögen quarry, Skövde, south central Sweden; Skövde-Vikarby Limestone.

Material. 100 specimens representing all the representative types of Pa and Pb elements of the species (58 Pa, 42 Pb).

Description. In this description the posterior process is used as reference and placed vertically when observed in oral view.

The Pa elements have four (sinistral elements) and up to five (dextral elements) branches, respectively. They have a blade-like anterior process and a long posterior process that is straight to slightly laterally bent when observed in upper view. Both sinistral and dextral Pa element have a large bifid antero-lateral process and a pointed to sub-rounded, short outer postero-lateral process forming an angle of 90° with the main denticle row and situated to the opposite side of the bifid process.

The anterior process is fully denticulate; it is straight in oral view, blade-like and arched in lateral view. The fused and blade-like denticles on the anterior process become tallest at about mid-length of the process. The posterior process is long and is fully denticulate. The long branch of the bifid antero-lateral process is fully denticulate and forms an angle of c.85 to 90° with the short lobe of the antero-lateral process. The anterior lobe of the bifid antero-lateral process is short, pointed and anteriorly directed. The postero-lateral process is short, wide and distally blunt in most specimens with one to four denticles forming an angle of 90° with the cusp and the main denticle row. The postero-lateral process is offset from the main denticle row in a distance at about two denticles behind the cusp. The basal cavity is well-developed and recessive; it is open (scaphate) below the cusp, The basal cavity of the anterior process is a slit with a recessed basal cavity; below the anterior process it is a slit.

The dextral Pa element has an additional inner postero-lateral process-like flare of the base. It is a broad expansion of the posterior platform. This postero-lateral flare may develop denticles at about four denticles. The offset of this small denticle row process initiates at the fourth denticle behind the opposite postero-lateral and short process. The denticle row on this postero-lateral process is vertical to posteriorly directed forming an angle from acute to nearly 90° with the main denticle row of the posterior process. The sinistral Pa element is similar to the dextral Pa element, but the additional postero-lateral process is not developed.

The three branched (ambalodiform, pastinate and semiplanate) Pb elements have relatively short posterior and antero-lateral processes. The anterior process is long and pointed and the short to shortest lateral process is pointed and directed downward. The anterior process is the longest process of the three processes. The basal cavity is expanded below the cusp and at the initial part of the processes; distally it is developed as a slit.

In upper view the angle between the posterior process and lateral process of the dextral Pb element is about 90° and the lateral process is directed towards the posterior. The posterior and lateral processes are nearly even in length. The angle between the lateral and anterior processes is nearly 180°.

Remarks. Ambalodus reclinatus Fåhræus, 1966 (Fåhræus 1966) is the sinistral Pb element. Viira (1974) introduced the form species *Polyplacognathus ramus*, which is the dextral Pa element of *E. reclinatus*.

Bergström (1971, pl. 1, figs 11–13) illustrated sinistral and dextral Pb elements and the dextral Pa element, which has a straight outline in upper view. The Pa elements here assigned to *E. reclinatus* (Fåhræus) are characterised by having the short, pointed to rounded postero-lateral process offset from the main denticle row by c.90°. This is identical to the dextral Pa element illustrated by Bergström (1971, pl. 1, fig. 13). The development of the additional flare to postero-lateral process varies from a minor bulge to a denticulate process forming an inclination from c.50 to 90° with the main denticle row. Bergström (1971) did not illustrate the sinistral Pa element.

Viira (2011) and Mellgreen *et al*. (2012) referred similar Pa elements to the species *E. foliaceus*, however their illustrated specimens are here assigned to *E. reclinatus*.

Occurrence. Present in all Bellewstown sections and also recorded from the samples of the lower Tramore Limestone Formation. This taxon also occurs together with *E. robustus* and cf. *E. robustus*.

Distribution. The taxon is common and has been recorded from several locations in the Baltic Palaeobasin of Baltica (e.g. Bergström 1971; Viira 1974, 2011; Zhang 1998b; Stouge *et al*. 2016b). Lehnert *et al*. (1999b) and Heredia *et al*. (2015, 2019) recorded the species from the San Rafael Block of the Cuyania Composite Terrane, Mendoza Province, western Argentina. It is the index species for the *Eoplacognathus reclinatus* Conodont Subzone of the *Pygodus serra* Conodont Zone.

Eoplacognathus robustus Bergström, 1971

Fig. 4.1–4.11

1971 *Eoplacognathus robustus* n. sp. Bergström, pp 140–1 (*cum syn*. up to 1971), pl. 1, figs 14–16

1974 *Eoplacognathus robustus* Bergström, 1971; Viira, pp 79–81, pl. VIII, figs 16–18, 88–92

1974 *Polyplacognathus robustus* (Bergström, 1971); Viira, pp 108–10, pl. IX, figs 3–9, 13–18, 137–8

1976 *Eoplacognathus lindstroemi robustus* Bergström; Dzik, text-fig. 32A–C

1985 *Eoplacognathus robustus* Bergström; Sevastopulo *in* Bergström and Orchard, p. 46, pl. 2.2, figs 8, 12

1994 *Eoplacognathus robustus* Bergström, 1971; Dzik, p. 98 (*cum syn.*), pl. 21, figs 3–5, text-fig. 23

1998 *Eoplacognathus robustus* Bergström; Heredia, p. 341, pl. I, figs 3-11, text-fig. 3

1998a *Baltoplacognathus robustus* (Bergström); Zhang, p. 54, pl. 8, figs 7–10

1998b *Baltoplacognathus robustus*; Zhang, pp 10–11, figs 7H–N, 11B2

1999b *Eoplacognathus lindstroemi* (Hamar 1964) early form; Lehnert and Bergström, pl. 2, figs 1–4

1999 *Baltoplacognathus robustus* (Bergström); Stouge and Bagnoli, pl. 2, figs 9–12

2008 *Baltoplacognathus robustus* (Bergström); Viira, p. 13, fig. 9F, F-1

2011 *Baltoplacognathus robustus* (Bergström); Viira, p. 13, fig. 9F

2012 *Baltoplacognathus robustus* (Bergström); Hints *et al.*, fig. 5D‑F

2013 *Eoplacognathus* sp. Tolmacheva, Zaitsev and Alekseev, pl. 1 (*pars*), figs 21–2, ?23

2015 *Eoplacognathus robustus* Bergström; Heredia and Mestre, pl. 1, figs 7, 8, 10, 11 (only)

2016a *Baltoplacognathus robustus* (Bergström); – Wu, Stouge, Zhan, Liu and Liang, fig. 3:6

2016b *Eoplacognathus robustus* (Bergström) - Wu, Calner and Lehnert, fig. 6b, c

2016b *Baltoplacognathus robustus* (Bergström); Stouge *et al.*, fig. 3H–I

2019 *Eoplacognathus robustus* Bergström; Heredia and Mestre, p. 560 (*pars*), fig. 3A–B, E–F, H–I.

2019 *Eoplacognathus robustus* Bergström; Heredia *et al*., fig. 3A, C, D–K.

Type locality and horizon. Gullhögen quarry, Västergötland, Sweden; 4m below top of the Gullhögen Formation (Llanvirn; Uhaku; Darriwilian; Middle Ordovician).

Material. 125 specimens (65 Pa and 60 Pb).

Description. In oral view the Pa elements comprise both straight and laterally bent forms. The holotype specimen of *Eoplacognathus robustus* Bergström, 1971 (pl. 1, fig. 16) is the dextral Pa element and the anterior and posterior process form a straight line in upper view. The short postero-lateral process is blunt and wide; it makes an angle of 70–80° with the main denticle row and thus is directed towards the anterior. An additional postero-lateral flare is developed on the posterior process; it often carries two to three denticles starting at the two denticles behind the short postero-lateral process. The additional postero-lateral process makes an acute angle to the main denticle row in a posterior direction. The anterior process is blade-like forming an arc in lateral view.

The dextral Pb element is Y-shaped and the sinistral Pb element is nearly T-shaped in oral view. The anterior process of both elements is longest and at least twice as long as the two other processes. In upper view the angle between the posterior process and the anterior process of the sinistral Pb element is of 100–110° and the lateral process makes and angle of about 100° with the posterior process. In the dextral Pb element the anterior process makes an angle of nearly 150° with the posterior process. The basal cavities of the Pb elements are narrow grooves that extend beneath the three processes. These specimens are fully described by Bergström (1971).

Remarks. Some specimens are easily assigned to *Eoplacognathus robustus sensu* Bergström, 1971, where the dextral Pa element has a straight outline in upper view. Laterally bended elements are included (see also Zhang 1998b,c). Except for the inclusion of the laterally curved elements the concept of this species follows strictly that of Bergström (1971, pl. 1, figs 14–6). *Eoplacognathus lindstroemi* early form *sensu* Lehnert and Bergström *in* Lehnert *et al*., 1999 shares the characters with the Bellewstown specimens assigned to *E. robustus*.

Dzik (1994) recorded a '*E. reclinatus–E. robustus*' transition in the lower *E. robustus* Zone from the Mójcza Limestone, Holy Cross Mountains, Poland. The two species occur together in the

Tramore samples Tram 10–12, the Bellewstown West samples and float sample #75 at Bellewstown and probably represent the coeval interval to the 'transitional fauna' in Poland.

Occurrence. Recorded from Bellewstown sections (Tables 1–3) and samples Tram 10, 12 from the lower Tramore Limestone Formation.

Distribution. This species is nearly globally distributed. It is common in the Baltoscandian region and is characteristic of the succession of the Mendoza province, eastern Argentina. It is found in deeper-water deposits in South China (Zhang 1998b,c), whereas the coeval interval on the platform in China is characterised by *Yangtzeplacognathus protoramosus* (Zhang 1998a,b,c). *E. robustus* is the subzonal index species of the *E. robustus* Conodont Subzone of the *Pygodus serra* Conodont Biozone (upper Darriwilian; Llanvirn; Middle Ordovician).

Eoplacognathus cf. *E. robustus* Bergström, 1971

Fig. 4.12–4.15

1974 *Ambalodus robustus* Bergström, 1971; Viira, pp 79–80 (*pars*), pl. 8, fig.17; text-figs 88, 90, 92 (*pars*).

Material. 144 specimens (68 Pa and 76 Pb).

Remarks. Some Bellewstown elements differ from commonly illustrated Pa and Pb elements of *E. robustus.* In the dextral Pa element, the additional postero-lateral flare initiates about four denticles behind the short postero-lateral process (= *reclinatus* character). In contrast at *E. robustus* the offset has moved towards the cusp and initiates about two denticles to the posterior of the short postero-lateral process. The short, tongue-like postero-lateral process makes an angle of 100° (= *robustus* character) with the posterior process. The sinistral Pa element does not deviate from that of *E. robustus*. The Pb elements are similar in morphology to the Pb elements of *E. robustus*, but the long anterior process makes an angle of 90° with the posterior process.

Aside from these differences, the Bellewstown specimens here referred to as *Eoplacognathus* cf. *E. robustus* are largely similar to *Eoplacognathus robustus sensu* Bergström, 1971. Some of the elements referred to *Ambalodus robustus* by Viira (1974) belong to this taxon also. She also illustrated the Pb elements of *E. robustus sensu* Bergström, 1971 (fig 17; text-fig. 88, 90).

Whether differences in the angles between the processes of the individual elements is a robust species character, or simply a reflection of intraspecific variation in the P elements of *Eoplacognathus robustus* remains an open question.

Occurrence. Present in all Bellewstown localities and in the upper two samples in the Lower Tramore Limestone Formation.

Distribution. Similar forms have been recorded from Estonia and the San Raphael, Mendoza Province, Argentina.

Genus PANDERODUS Ethington, 1959

Type species. Paltodus unicostatus Branson and Mehl, 1933.

Remarks. The apparatus of *Panderodus* Ethington, 1959 has been reconstructed by several authors (e.g. Sweet 1979; Jeppsson 1983; Fåhræus and Hunter 1985; Sansom *et al*. 1994).

Panderodus sulcatus (Fåhræus, 1966)

Fig. 5.5–5.8

1966 *Paltodus sulcatus* n. sp. Fåhræus, p. 25, pl. 3, fig. 9a,b

1966 *Panderodus gracilis* (Branson and Mehl); Fåhræus, p. 26, pl. 3, fig. 14a,b

1976 *Panderodus gracilis* (Branson and Mehl); Dzik, p. 435, text-fig 15a,b (only)

1978 *Panderodus sulcatus* (Fåhræus); Löfgren, p. 67, pl. 8, figs 7–9

1981 *Panderodus* cf. *P. gracilis* (Branson and Mehl, 1933); Nowlan p. 12, pl. 1, figs 14, 17, 18

1985a *Panderodus gracilis* (Branson and Mehl, 1933); Fåhræus and Hunter, text-fig. 1

cf. 1987 *Panderodus* sp. Bauer, p. 23, pl. 4, fig. 12

1994 *Panderodus sulcatus* (Fåhræus); Dzik, p. 59 (*cum syn*.), pl. 12, figs 21–28; pl. 24, fig. 1, text-fig. 3a

1998c *Panderodus sulcatus* (Fåhræus); Zhang, pp 78–9 (*cum syn*.), pl. 13, figs 1–5

2001 *Panderodus sulcatus* (Fåhræus, 1966); Rasmussen, p. 104, pl. 12, figs 4–5

2001 *Panderodus sulcatus* (Fåhræus); Viira *et al*., fig. 9l

2008 *Panderodus sulcatus* (Fåhraeus); Viira, fig. 3S,T

2012 *Panderodus sulcatus* (Fåhræus); Hints *et al*., fig. 6A

2012 *Panderodus sulcatus* (Fåhræus, 1966); Mellgren *et al*., figs 5AE–AF

2013 *Panderodus sulcatus* (Fåhraeus, 1966); Tolmacheva *et al*., p. 397, pl. II, figs 32–34

2018 *Panderodus sulcatus* (Fåhræus, 1966); Bergström and Ferretti, fig. 6V,X

Type locality and horizon. The Gullhögen quarry, Västergötland, Sweden; Skövde Limestone, *Eoplacognathus reclinatus* Conodont Subzone of the *Pygodus serra* Conodont Zone (Darriwilian).

Material. 423 specimens.

Remarks. The slender S elements are straight to gently bowed. Other than this, the Irish material conforms the description of the species provided by previous authors.

Occurrence. Present and common in the investigated samples from both the Bellewstown Limestone Member and from the Tramore Limestone Formation (Tables 1- 4).

Distribution. *Panderodus sulcatus* is a pandemic species recorded from Baltica, South China, Wales and now also eastern Ireland.

Genus PLECTODINA Stauffer, 1935

Holotype. *Prioniodus aculeatus* Stauffer, 1930.

Remarks. Seven morphologically different specimens are here assigned to the genus *Plectodina*: angulate pastinate Pa, bipennate Pb, geniculate coniform M, alate Sa, breviform digyrate Sb, dolobrate Sc and dolobrate Sd elements. The genus *Nordiora* Rasmussen, 2001 shares the P elements with same or almost same morphology as the genus *Plectodina*. However, the M and S elements assigned to the genus *Nordiora* by Rasmussen (2001) are different and the genera are not considered to be identical. Two informally defined species, *Plectodina* sp. A from the lower Tramore Limestone and *Plectodina* sp. B from Bellewstown Limestone, are distinguished here.

Plectodina sp. A

Fig. 5.14–5.18

cf. 2018 *Plectodina flexa* (Rhodes, 1953); Bergström and Ferretti, fig. 6q–r

cf. 2018 aff. *Microzarkodina* sp. Miller *et al.*, pp 585, 586, fig. 9

2022 aff. *Plectodina flexa* (Rhodes, 1953); Ferretti and Bergström, p. 482, fig. 9P–A'; *non* fig. 12J–R (= *P. flexa* in figure caption, but should be *Plectodina* sp. Ferretti and Bergström, p. 482)

cf. 2023 *Microzarkodina* sp. Heward *et al.*, p. 13, fig. 10F

?2023 *Nordiora* sp.; Heward *et al.*, fig. 10G–H.

?2023 indet.; Heward *et al.*, fig. 10E, ?I.

Material. 121 specimens comprising 50 Pa, 7 Pb, 26 M, 10 Sa, 3 Sb, 22 Sc and 4 Sd elements.

Description. The pectiniform Pa element is straight in upper view and angulate in lateral view. The anterior process is longer and higher than the posterior process. Both processes are with closely spaced but discrete and apically free denticles. Denticles are laterally compressed and with white matter. The suberect cusp is prominent, well-developed and keeled. The basal cavity is open beneath the main cusp forming a flare; distally the cavity becomes shallow on the processes. The Pb element is pastinate with a prominent suberect cusp. It is keeled and with a triangular base. The basal cavity is open. The upper margin is broken but appears to be adentate.

The M element is geniculate with a reclined cusp and a long extended anticusp and the symmetrical Sa element is breviform alate with discrete denticles on the lateral processes. The Sa cusp is relatively narrow and its basal cavity is shallow and extends the full length of the processes. The Sb element is breviform digyrate, with a prominent lateral keel/costa on the convex side. The Sb cusp is long, and the basal cavity is narrow and extends the full length of the processes. The dolobrate Sc element is laterally compressed with inclined denticles on the upper margin of the base and on the posterior process. The anterior short process is adentate and the cusp is recurved.

Remarks. Sd element for this taxon have only been recorded as fragments. Specimens described from the Amdeh Formation, Oman (Heward *et al*. 2023; Miller *et al*. 2018) share similarities with the specimens from the Tramore Limestone Formation. However, the state of preservation of the Oman specimens generally does not permit precise species identification. It is however considered possible that the Oman specimens are conspecific with *Plectodina* sp. A.

P. flexa (Rhodes, 1953) *sensu* Bergström and Ferretti (2018) and Ferretti and Bergström (2022) from Wales (Avalonia) shares the composition of the apparatus and the same elements included. The large extensive and open basal cavity of the Pa elements and the denticulate M element separates *Plectodina flexa* from *P.* sp. B. Comments to the difference between *Plectodina* sp. A and *P.* sp. B are given with discussion of the latter species.

Occurrence. *Plectodina* sp. A is recorded from the lower Tramore Formation.

Distribution. So far, *Plectodina* sp. A is known from southeast Ireland; however, the species may also be present in the Amdeh Formation, Wadi Daiga, Oman.

Plectodina sp. B

Fig. 5.19–5.29

cf. 1999 *Bryantodina* n. sp. A Lehnert and Bergström; Lehnert *et al*., pl. 1 figs 12, 16, 18. 19

cf. 2022 *Plectodina* sp. Ferretti and Bergström, p. 482, fig. 12J–R

Material. 1373 specimens (149 Pa, 203 Pb, 152 M, 256 Sa, 97 Sb, 426 Sc and 90 Sd).

Description. The pectiniform Pa element is arched to angulate and scaphate. The large anterior process is high and blade-like with prominent sharp-edged denticles; the bladelike process is downwardly directed. The posterior process of the Pa is bar-like and denticulate. The Pb element is pastinate and has large, rounded, anteriorly and posteriorly keeled cusp with inner-lateral costa. The anterior keel produced basally as short, adenticulate, downwardly projecting process. The lateral and posterior anterior processes are fully denticulate, and the basal opening of the Pb is wide.

The M element is geniculate coniform, with a laterally compressed, anteriorly and posteriorly keeled cusp. The anterior keel is developed basally as a pointed anterior and downwardly projected adenticulate extension of the base. The posterior upper margin of the M element is keeled that extends posteriorly as a posterior process.

The Sa element is alate to tertiopedate. The cusp is rounded but with lateral costae and the posterior process is broken in most specimens, when preserved it is long. Laterally processes are directed downward with laterally compressed and free denticles. The Sa elements are symmetrical, but a few specimens are slightly asymmetrical due to one lateral branch may be shorter than the other. The tertiopedate Sb element has a prominent outer lateral costa on the cusp that continues downward as a denticulate lateral process. The anterior keel of the cusp extends into the antero-lateral denticulate process. The dolobrate Sc element has a triangular base in lateral view; denticles are free and well displayed on the upper margin of the base and the posterior process. The Sd element is bipennate; its anterior process is adentate and short; it is turned laterally. The posterior process of the Sd is long, straight and with a series of thin laterally compressed denticles.

Remarks. The posterior process of the Sa element is often broken, but when preserved it is of similar length as the lateral processes. The Pa element of *Plectodina* sp. B is similar to *Bryantodina* sp. A illustrated by Lehnert and Bergström (1999) and could be conspecific or at least closely related to *Plectodina* sp. B. Additional elements that potentially belong to the *Plectodina* apparatus were not illustrated by Lehnert and Bergström from the Argentinian material.

Plectodina sp. B is distinguished from *Plectodina* sp. A by the specimens which have large open basal cavities, or are nearly scaphate, whereas in *Plectodina* sp. A, the elements are more planate. The Sa element of *Plectodina* sp. A is alate, however it is tertiopedate in *Plectodina* sp. B. The general aspect of *Plectodina* sp. A highlights the robustness of the elements, whereas the specimens of *Plectodina* sp. A have a more 'elegant' aspect.

Occurrence. Present to common in most samples from the Bellewstown Limestone Member, eastern Ireland.

Distribution. Known from east Ireland; perhaps also present at the San Rafael block of the Cuyania Terrane and in northeast Oman.

Genus SAGITTODONTINA Knüpfer, 1967

Type species. *Sagittodontina robusta* Knüpfer, 1967.

Recognised species. *Sagittodontus* sp. A, *Sagittodontina kielcensis* (Dzik, 1976), *S. sanrafaelensis* (Lehnert and Bergström, 1999) and *S. robusta* (Knüpfer, 1967).

Sagittodontina sanrafaelensis (Lehnert and Bergström, 1999)

in Lehnert *et al*., 1999

Fig. 3.20–3.27

Holotype. Amorphognathus sanrafaelensis Lehnert and Bergström *in* Lehnert *et al*., 1999.

1994 *Sagittodontina kielcensis* (Dzik, 1976); Dzik, p.88 (*pars*), pl. 22, fig 4 (only)

1999b *Amorphognathus sanrafaelensis* n. sp. Lehnert and Bergström *in* Lehnert *et al.*, pp 208, 210, pl. 1, figs 1–3, 5–6, 8–9

1999a *Amorphognathus kielcensis* Dzik, 1976; Lehnert *et al.*, pl. 1, figs 1, 4, 6–7

?1999c *Saggitodontinas kielcensis* Dzik; Zhang, p. 88 (*pars*), pl.16, figs 9–11, 13

Type locality and horizon. San Rafael, Mendoza Province, west-central Argentina. Peletay Member of the Lindero Formation, type section of the Lindero Formation.

Material. 57 elements represented by Pa, Pb, M, Sa and Sb elements.

Remarks. Lehnert and Bergström (1999) described the Pa, Pb, M and Sa elements of this taxon. Additional S elements are recorded and illustrated by Zhang (1999c) and here. The morphology of the Pa elements changes with size (Lehnert and Bergström 1999). Small(er) specimens are not species diagnostic, whereas the large (or ontogenetically mature) are. The Pa element from the *E. robustus* Zone and assigned to *S. kielcensis* (Dzik 1994) may well belong to this species. Pa elements show the pronounced lateral expansion on the proximal part of the posterior process as described by Lehnert and Bergström (1999). On medium-sized specimens this expansion is developed as a lateral shoulder. The Pb element characteristically has a widely excavated antero-lateral process on mature specimens.

S. sanrafaelensis is here considered the ancestor of, and is succeeded by, *S. kielcensis* Dzik, 1976 in the *Eoplacognathus lindstroemi* Subzone ranging into *Pygodus anserinus* Zone. Commonly, *S. rafaelensis* has been assigned to *S. kielcensis* Dzik by previous authors (e.g. Dzik 1994; Lehnert *et al*. 1999a; Zhang 1999c). However, the prominent shoulder and widely excavated and deep basal cavity of the pectiniform specimens are characteristics of *S. sanrafaelensis*, These characters are much less prominent in the Pa elements of *S. kielcensis*.

Occurrence. Samples from Bellewstown Limestone Member, eastern Ireland.

Distribution. This species is recorded from the Peletay Member of the Lindero Formation, Mendoza Province, Argentina (*Eoplacognathus reclinatus* Subzone of the *Pygodus serra* Zone). It is present in the Folkeslunda Limestone, Sweden in the *Yangtzeplacognathus foliaceus* Conodont Zone with a range into the *Eoplacognathus reclinatus* Subzone of the *Pygodus serra* Conodont Zone. In the Yichang area, South China it is present in the uppermost part of the Kuniutan Formation (*Yangtzeplacognathus protoramosus* Conodont Zone; unpublished own observation).

Conodont biostratigraphy

Pygodus serra, *Eoplacognathus reclinatus* and *E. robustus* are the biostratigraphically important taxa in the conodont fauna from eastern and southeastern Ireland (Fig. 6). Additional taxa significant for correlation include *Baltoniodus alatus* (Hadding), *Periodon aculeatus* (Hadding), *Plectodina* spp, and *Sagittodontus sanrafaelensis* (Lehnert and Bergström). The *Pygodus serra* Conodont Zone is identified based on the presence of the nominate species *Pygodus serra. The Eoplaognathus reclinatus* Conodont Subzone is identified based on the presence of *Eoplacognathus reclinatus* and the succeeding *Eoplacognathus robustus* Conodont Subzone is determined based on the appearance of *Eoplacognathus robustus* in the samples.

Eoplacognathus reclinatus and *E. robustus* are the index fossils for two conodont subzones of the *Pygodus serra* Conodont Zone (following Bergström 1971). The former species is found the lower samples of the lower Tramore Limestone Formation and also the Bellewstown Limestone Member, in which *Sagittodontus sanrafaelsensis* also occurs. *Eoplacognathus robustus* appears together with *Pygodus serra* in the samples of Bellewstown East and West and in the samples Tram 12 and Tram 14 (= 14 m above the base) from the Tramore Limestone Formation. Both species occur together in the float samples representing a '*reclinatus-robustus* transition' of the basal *E. robustus* Conodont Subzone. *Pygodus serra* is sporadically represented and is recorded from samples BellWest 12, float sample BellN 75 and from Tram 14 (Tables 1–4). The assemblage is late Darriwilian (Dw3; Middle Ordovician; late Llanvirn; Fig. 6).

Correlation

Regional correlation

The Bellewstown Limestone Member and lower Tramore Limestone Formation are clearly coeval deposits as significant biostratigraphic zonal index taxa are shared (Fig. 7). Several genera and species are common with the conodont fauna from South Wales, UK, described by Ferretti and Bergström (2022). The frequent record of *Eoplacognathus lindstroemi* in the conodont fauna from Wales suggests that it is younger than the conodont fauna recorded here from eastern/southeastern Ireland. *E. lindstroemi,* however, is reported from the Tramore Limestone Formation (Brenchley *et al*. 1977; Bergström 1971; Bergström and Orchard 1985), suggesting that the deposits at Tramore, and probably also the Bellewstown Limestone, reach into younger levels than directly recorded and investigated here.

A difference between the Tramore and Bellewstown samples is the lack of *Sagittodontina* in the Tramore Limestone Formation (Tables 1, 4), but perhaps with a better yield from this particular unit such difference may disappear. The presence of *Plectodina* sp. A from Tramore vs *Plectodina* sp. B at Bellewstown is another conspicuous difference between the two areas.

Intercontinental correlation

Correlation of the *Pygodus serra* Conodont Zone and the two subzones has been outlined by many authors (Bergström 1971, 2007a,b and Goldman *et al*. 2023 with references) and will not be repeated here, but a few selected areas are discussed (Fig. 7):

Argentina. Correlation with the Precordillera, Argentina, using conodonts is not easy as the coeval strata are developed in shaley facies. *Eoplacognathus reclinatus, E. robustus* and *Sagittodontina sanrafaelensis* occur together in the siliciclastic dominated succession deposited on the San Rafael

Block of the Mendoza province, Argentina (i.e. 'Cuyania Composite Terrane'). These strata rest - unconformably on Mesoproterozoic basement rocks and consist mainly of siliciclastic calcareous sandstone and quartz sandstone mixed with minor limestone horizons and beds (Lehnert *et al*. 1999; Heredia and Mestre 2019; Heredia *et al*. 2015, 2019). Associated taxa are *Baltoniodus alatus, Periodon aculeatus, Plectodina* sp. B and *Protopanderodus varicostatus*. The San Rafael strata extend into the *Pygodus anserinus* Zone (Lehnert *et al*. 1999: Heredia *et al*. 2019 and references therein). Part of the San Rafael fauna correlates with the Bellewstown conodont fauna (including material from float samples). The Argentinian succession and its fauna is similar to the lower Tramore Limestone succession and fauna and also correlates with the middle and upper part of the Tramore Limestone Formation.

Baltoscandia. The Bellewstown and Tramore faunas share the significant biostratigraphic taxa *Eoplacognathus reclinatus*, *E. robustus*, *E. lindstroemi* and *Pygodus serra* with the conodont fauna from the Baltic palaeobasin (Bergström 1971, 2007b) and southern Poland (Dzik 1976, 1978, 1994) (Figs. 6–7). The fauna correlates with the *Baltoplacognathus reclinatus*, *B. robustus*, *Y. protoramosus* and *pars E. lindstroemi* Conodont zones of Männik and Viira (2012). This is Darriwilian (Dw3) (Middle Ordovician) corresponding to the Lasnamägi-Uhaku stages of the Baltic Regional System (Fig. 6; Meidla *et al*. 2014; Meidla 2023) and the Segerstadian Stage of the Scandinavia Regional System (Nielsen *et al*. 2023). *Baltoniodus alatus, Periodon aculeatus, Sagittodontina sanraphalensis* and *Triangulodus alatus* are also shared with the Baltoscandian conodont fauna.

Intra–Iapetus correlation. Occurrences in central Newfoundland comprise the well-known Cobbs Arm Limestone and its lateral equivalent locations on New World Island in the Exploits Subzone (Bergström 1971; Bergström *et al.* 1974; Stouge 1980a,b; Fåhræus and Hunter 1981, 1985a,b; Nowlan 1984; Nowlan and Neuman 1995). The Cobbs Arm Limestone is the lower formation of the

Hillgrade Group. It overlies volcanic rocks of the Summerford Group and is overlain by the shales of the Rodgers Cove Formation, yielding graptolites of the *Nemagraptus gracilis* Zone (Sa1, Sandbian; Upper Ordovician) (Erdtmann 1971; Bergström *et al*. 1974). The conodont fauna from the Cobbs Arm Limestone includes the index species *Eoplacognathus robustus*, *E. lindstroemi*, *Pygodus serra* and *Pygodus anserinus*. Additional taxa in common with southeastern Ireland are *Baltoniodus alatus*, *Periodon aculeatus* and *Protopanderodus varicostatus*. The Cobbs Arm Limestone deposited during *Pygodus serra* and *P. anserinus* times (top Darriwilian, Dw3 to early Sandbian; late Middle–early Late Ordovician; Llanvirn–Llandeilo).

An additional record of a coeval limestone deposit yielding conodonts and shelly fossils is known from the Gander area on the Avalonia Peninsula, Newfoundland (Stouge 1980a,b; Nowlan 1981; Nowlan and Newman 1995). The conodont fauna is recorded from fossiliferous limestone exposed near and east of Gander on the Avalon Peninsula, Newfoundland and within the Davidsville Group (Stouge 1980a,b, 1981; Blackwood 1982; Boyce *et al*. 1988; Nowlan and Newman 1995). The Davidsville conodont fauna includes *Eoplacognathus robustus* and *Eoplacognathus lindstroemi* associated with *Baltoniodus alatus*, *Periodon aculeatus* and *Protopanderodus varicostatus* (Stouge 1980a). Thus, the Davidsville conodont fauna is partly coeval with the conodont fauna recovered here from the Bellewstown Limestone Member and the upper lower into middle Tramore Limestone Formation.

Laurentia. The common presence of *Plectodina* spp. in the samples should, in principle, provide a potential for correlation to the biozonation of North America midcontinent (Goldman *et al*. 2023), but the two species *Plectodina* A and B are different from those known from that region. Thus, a direct correlation with North America is not possible at this stage based on the present fauna.

South China. The two species of *Eoplacognathus* recorded here are rare to practically absent in the successions of South China (e.g. Zhang 1998c). In the late Darriwilian an incomplete provincial barrier existed in South China and the records of *E. reclinatus* and *E. robustus* are from deeper-water deposits at the margin of the South China platform (An 1987; Zhang 1998c; Wu *et al*. 2016). Instead, the *Yangtzeplacognathus* lineage evolved on the platform and dominated the fauna of South China (Zhang 1998b,c). Records of *Pygodus serra* from South China (Zhang 1988a,c) provide correlation between southern Ireland and South China. However, and interestingly, *Sagittodontina sanrafaelensis* occurs together with *Baltoniodus alatus*, *Periodon aculeatus*, *Protopanderodus varicostatus* and *Triangulodus alatus* in the *Yangtzeplacognathus protoramosus* Conodont Zone suggesting (*pars*) correlation of this latter regional biozone to the *E. reclinatus* and *E. robustus* subzones of Bellewstown and Tramore (Fig. 6).

Oman. *Plectodina* sp. A and *Drepanoistodus* sp. A are shared with the fauna from Oman (Miller *et al.* 2018; Heward *et al.* 2018, 2023) suggesting some time equivalent between the Tramore Limestone Formation and Amdeh Formation of Oman. The record from Oman of *Yangtzeplacognathus protoramosus,* which is a taxon known from the *Pygodus serra* Zone, is an indirect support to this correlation.

Palaeoecology and biofacies

Conodont biodiversity. 16 species and four taxa in open nomenclature are identified from the deposits of the Bellewstown Limestone Member and Tramore Limestone Formation. Conodont species diversity shows significant changes from the *Eoplacognathus reclinatus* Conodont Subzone to the *Eoplacognathus robustus* Conodont Subzone. Representatives of *Plectodina* and *Panderodus* have a more continuous record compared to all other taxa. Peak in diversity (with 13 species) occurs in sample BellEast 4, and with 11 species in samples BellWest 11 and BellWest 12, this correlates with the beginning of the *E. robustus* Zone.

Conodont biofacies. The general conodont faunal succession of the lower Tramore Limestone Formation and most of the samples of the Bellewstown Limestone Member have *Panderodus* and *Plectodina* as the dominant genera. *Belodella* and *Drepanoistodus* sp. A also occur but are numerically subordinate. *Baltoniodus* and *Eoplacognathus* become common in samples from Bellewstown West and the float sample from the Bellewstown locality A.

Analysis of the conodont taxa from Ireland shows that the *Plectodina* association dominates the *Eoplacognathus reclinatus* Subzone of the section (Figs 8–9). At Bellewstown the *Plectodina* association is recorded from the samples in the Bellewstown East samples. Some samples from Bellewstown West document a transition to the *Baltoniodus* association (Fig. 9). The relative abundance of *Baltoniodus* and *Eoplacognathus* conodonts is higher than *Panderodus* and *Plectodina* combined in the Bellewstown West samples 12 and 13 and is responsible for the shift in conodont biofacies (Figs 8–9).

The results from conodont biofacies analysis suggest changing bathymetric conditions from the *Eoplacognathus reclinatus* Subzone to *E. robustus* Subzone. Generally, the *Plectodina* association is characteristic of shallow-water inner shelf depositional conditions in the *E. reclinatus* Subzone. A second association consists of the addition of the genus *Baltoniodus* – a taxon that is characteristic of relatively more offshore shelf environs (Rasmussen and Stouge 2018). *Eoplacognathus* becomes frequent in the BellWest 12 and 13 and the BellN 75 samples, forming a third association. It is associated with *Baltoniodus* and *Sagittodontina*; *Plectodina* occurs in low numbers and *Periodon* and *Pygodus* are rare to present. The latter two genera are open oceanic faunal elements and widely spread along margins of and within the Iapetus Ocean (Bergström and Carnes 1976; Stouge 1984; Rasmussen and Stouge 1993, 2018).

The late Darriwilian conodont faunal succession from both Bellewstown Limestone Member and the lower Tramore Limestone Formation show a trend from shallow-water (i.e. *Belodella*, *Panderodus* and *Plectodina*) to temperate-water faunas, with traces of open marine faunas in the younger strata. In the Tramore Limestone Formation this trend is reflected in the sedimentology of the sequence, i.e. conglomeratic facies (unit 1), which is successively overlain by silty limestone (unit 2) and then shale and nodular limestone (unit 3). The pattern relates well with the proposed shallow-water inner shelf environment for the lower Tramore Limestone Formation (units 1 and 2 *pars* of Carlisle 1979). The *Baltoniodus* and *Eoplacognathus* associations relate well with the sediments of moderate energy and relative deeper water environment (unit 2 into unit 3 of Carlisle 1979).

Palaeogeographical affinities and significance of the fauna

The provincial signal of the *Plectodina*-dominated conodont fauna from east and southeastern Ireland is shared with the San Rafael Block, Mendoza Province, Argentina and South Wales (Figs 10, 11). The genus is not recorded from Baltica and South China in the late Darriwilian but is well represented in South Wales part of the Avalon Terrane (Rhodes 1953; Ferretti and Bergström 2022) and perhaps also from and perhaps also with the Sultanate of Oman (see Miller *et al*. 2014). The appearance of the genus in North China and on Laurentia was later (i.e. Sandbian) than recorded here from east and southeastern Ireland. The mixed influence by other taxa suggests that provincialism existed to some degree, but the barrier was perforated causing a complex pattern of spreading and communication.

The *Plectodina* association displays marked peri-Gondwana and Gondwana provincial affinities (cf. Dzik 1989; Miller *et al*. 2014), suggesting that the Bellewstown Subterrane must have lain in the south Iapetus Ocean, close to the Leinster Terrane or at least at higher latitudes in the Middle Ordovician (Figs. 10, 11). Additional but forming a smaller fraction of the fauna includes *Baltoniodus* and *Eoplacoplacognathus* of the North Atlantic Realm and these are shared with faunas of island arc/backarc settings within the Iapetus Ocean. *Belodella, Panderodus* and *Plectodina* show affinities to Wales or Gondwana (Figs 10, 11).

In the late Darriwilian the conodont fauna shows affinity to the well-known conodont faunal succession from Baltoscandia and from the Moscow Basin (Tolmacheva and Degtyarev 2022), where alongside the pandemic genera *Drepanoistodus, Pygodus, Periodon* and *Protopanderodus*, species of *Baltoniodus*, *Eoplacognathus, Gothodus* and *Sagittodontina* are shared. The presence of *Sagittodontina sanraphalensis* at Bellewstown (only) is significant, because the species is first recorded from the San Rafael Block of the Cuyania Composite Terrane, Mendoza Province of western Argentina (Lehnert *et al*. 1999). Since then, this taxon is recorded from the upper Kuniutan Formation of South China (SS own observation). Current evidence, therefore, suggest that it migrated from an origin in Peri-Gondwana to Gondwana, became widespread during the late Darriwilian, where it also reached Baltica (Stouge *et al*. 2020; Tolmacheva and Degtyarev 2022) and South China.

The Cobbs Arm Limestone and lateral equivalent from the Exploits Subzone of the Dunnage Zone, now distributed in eastern and northern central Newfoundland, formed island arcs along the leading edge of Ganderia. The increase of taxa that derived from Laurentia in the Cobbs Arm conodont fauna reflects a decrease of distance between the Laurentia and the Ganderia Terrane (Bergström *et al*. 1974; Stouge 1980a,b; Fåhræus and Hunter 1981, 1985a,b; Boyce and Ash 1988).

The general cold to temperate faunal assemblage from the Cuyania Composite Terrane includes also the genera *Ansella* and *Costiconus*. This is a similarity to the fauna of the Exploit Subzone and suggest that it occupied an intermediate position between Gondwana and Laurentia and perhaps communicated with areas such as Cobbs Arm Limestone of the Exploits Subzone.

Summary and conclusions

The conodont fauna investigated here from the Bellewstown Subterrane and the Leinster Terrane in east and southeast Ireland, respectively, includes genera that are characteristic of the North Atlantic Conodont Realm, whereas typical members of the Midcontinent Conodont Realm are absent.

The conodont fauna from the Bellewstown Limestone Member and Tramore Limestone Formation are nearly coeval. Both are assigned to the *E. reclinatus* and *E. robustus* Conodont Subzones of the *Pygodus serra* Conodont Zone (Middle Ordovician; Darriwilian, Dw3). The record of the younger index species *E. lindstroemi* from higher levels of the Tramore Limestone Formation has not directly been recorded in this investigation, but were previously documented by Bergström and Orchard (1985). The strata correlate with deposits from other terranes in Iapetus and palaeocontinents, whereas direct correlation to Laurentia platform and Precordillera Argentina is not possible. The Bellewstown Limestone Member is unique as it preserves *Sagittodontina rafaelensis* in the *E. reclinatus* Conodont Zone. The presence of *Sagittodontina sanrafaelensis* at Bellewstown - first recorded from the San Rafael block in Argentina - is also interesting, because the species is now identified from both Baltica and on the otherwise temporal provincially restricted South China Terrane and thus it provides means for precise correlation between these areas.

At Tramore, the general upwards deepening condition, provided an increase of communication with the open marine environment (Liljeroth *et al*. 2017). The pronounced sea-level rise noted at Tramore is reflected by the gradual appearance of open-marine conodont taxa such as *Periodon*, *Protopanderodus* and *Pygodus*. The initial transgression is marked by the appearance of *Eoplacognathus reclinatus* and characterised by the dominance of the *Plectodina* association. This association became mixed by the appearance of taxa with oceanic affinities such as *Drepanoistodus*, *Eoplacognathus*, *Baltoniodus*, *Periodon, Protopanderodus* and *Pygodus* (i.e. upper unit 2 into unit 3). A similar trend is recorded from the samples of the Bellewstown Limestone Member. At both locations, taxa with cool to temperate water preferences such as *Baltoniodus* and *Sagittodontina* arrived along with the first rise or in the ‘serra loop‘ comprising all of the *Pygodus serra* Conodont Zone of the overall larger late Darriwilian–early Sandbian global sea-level rise (Fig. 7; cf. Liljeroth *et al*. 2017).

The sea-level changes (described by Ross and Ross 1995; Liljeroth *et al*. 2017 with references) controlled the conodont evolutionary lineages including the *Baltoniodus*, *Eoplacognathus, Periodon* and *Pygodus* lineages. The *Eoplacognathus reclinatus-robustus-lindstroemi* lineage shows close connection to the first transgressive-regressive cycle (‘the serra loop’) in the early late Darriwilian (Fig. 7), when *E. reclinatus* appeared. It was followed by *E. robustus* (i.e. the *reclinatus–robustus* transition) and *Eoplacognathus robustus* evolved and became widely distributed during this first transgression. *E. lindstroemi* appeared and the early distribution of *E. lindstroemi* coincided with the following regressive but brief sea-level lowstand. It can be added that *Yangtzeplacognathus protoramosus* migrated from South China to Baltica in the post *E. robustus*–pre *E. lindstroemi* time (e.g. Männik and Viira 2012, fig. 1; Meidla *et al*. 2014).

Thus, the sea-level changes initiating during the late Darriwilian can explain the distribution patterns of *Belodella*, *Panderodus* and *Plectodina* in Ireland. The transgression is coeval with appearance and the wide distribution of *Pygodus serra.* It corresponded to the interval where the deposition more or less could keep pace the sea-level rise as seen in the succession of the lower Tramore Limestone Formation and at Bellewstown. This first transgressive–regressive loop corresponds with the narrow distribution of *Baltoniodus alatus*, *Periodon aculeatus*, *Sagittodontina sanrafaelensis* and *Plectodina* sp. A and B.

The Tramore Limestone Formation and Bellewstown Limestone Member conodont faunas suggest a palaeogeographic position of the Leinster and Bellewstown terranes, respectively, within a cool to temperate and/or mid-high latitudinal position in a peri-Gondwana setting (Figs 10–12). This palaeogeographic position is shared with the San Rafael block of the Cuyania Composite Terrane of Argentina where the conodont fauna is similar. *Plectodina* and *Yangtzeplacognathus* derived from east Gondwana and spread first to South China and further to Ireland and other peri-Gondwanan terranes. The fauna from easrtern/southeastern Ireland communicated with the Exploits Subzone and Baltica to some degree, which allowed for exchange of taxa between Baltic and further between South China (Fig. 12).

The brachiopod fauna from the lower Tramore Limestone Formation is associated with the Celtic Province (Harper and Parkes 1989, 1990; Liljeroth *et al*. 2017; Harper 2023). The *Plectodina* conodont association fits with the brachiopod facies FA–A and FA–B, respectively, of Liljeroth *et al*. (2017), although the resolution of conodonts does not allow a distinction between the FA–A and FA–B brachiopods facies.

The palaeogeographic distribution of brachiopods (Holmer *et al*. 2015, 2016; Liljeroth *et al*. 2017 with references) is shared by the conodonts from the same areas and terranes in the same time interval. This suggests that the palaeobiogeographic distribution displayed by the shelly fauna is also valid for the conodonts.

Acknowledgements

We are grateful for review comments from Stephen A. Leslie and John Murray that significantly improved the MS while giving us some pause for thought. John Murray is thanked for his high-quality editorial work that reshaped the MS in its final stages.

Svend Stouge thanks Kresten Anderskouv for making the SEM at the Department of Geosciences and Natural Resource Management, University of Copenhagen, Denmark available. The skilled help by Lako Blazik taking the SEM photos is gratefully acknowledged. David Harper thanks the Leverhulme Trust (UK) for support. Here we record our thanks to the late George Sevastopulo for his collection and many years of sage advice and friendship.

References

Albanesi, G.L., Monaldi, C.R., Barnes, C.R. and F.J. Zaballo 2023 An endemic conodont fauna of Darriwilian (Middle Ordovician) age from the Santa Gertrudis Formation, southwestern Gondwanan margin and its paleobiogeographic relationships. *Marine Micropaleontology* **181**, 102241, 1–21. https://doi.org/10.1016/j.marmicro.2023.102241

Aldrigde, R.J. 1982 A fused cluster of coniform conodont elements from the Late Ordovician of Washington land, western North Greenland. *Palaeontology* **25**, 425–30.

Aldrigde, R.J. and Purnell, M.A. 1996 The conodont controversies. *Tree* **11**, 463–8.

An, T-X. 1985. *The Lower Paleozoic conodonts of South China*. Publishing house of geology, Beijing, China, 238pp.

Bagnoli, G. and Stouge, S. 1997 Lower Ordovician (*billingenian–kunda*) conodont zonation and provinces based on sections from Horns Udde, North Öland, Sweden. *Bollettino della Società Paleontologica Italiana* **35**, 109–63.

Baily, W.H. 1865 Palaeontological notes, 18–30. In G.V. du Noyer (ed.), *Explanation to accompany sheets 167, 168, 178, and 179 of the maps, and sheet 13 of the longitudinal sections of the Geological Survey of Ireland*. Memoirs of the Geological Survey of lreland, Dublin.

Bauer J.A. 1987 Conodonts and conodont biostratigraphy of the McLish and Tulip Creek formations (Middle Ordovician) of south-central Oklahoma. *Oklahoma Geological Survey Bulletin* **141**, 1–58.

Bauer J.A. 1994 Conodonts from the Bromide Formation (Middle Ordovician), south-central Oklahoma. *Journal of Paleontology* **68**, 460–5.

Bergström, S.M. 1971 Conodont biostratigraphy of the Middle and Upper Ordovician of Europe and eastern North America, 83–161. In W.C. Sweet and S.M. Bergström (eds), *Symposium on Conodont Biostratigraphy*. Geological Society of America Memoir **127**.

Bergström, S.M. 1980 Conodonts as paleotemperature tools in Ordovician rocks of the Caledonides and adjacent areas in Scandinavia and British Isles. *Geologiska Föreningens i Stockholm Förhandlingar* **102**, 377–92.

Bergström, S.M. 1983 Biogeography, evolutionary relationships, and biostratigraphic significance of Ordovician platform conodonts. *Fossils and Strata* **15**, 35–58.

Bergström, S.M. 2007a Middle and Upper Ordovician conodonts from the Fågelsång GSSP, Scania, southern Sweden. *GFF* **129**, 77–82.

Bergström, S.M. 2007b The Ordovician conodont biostratigraphy of the Siljan region, south-central Sweden: a brief review of an international reference standard. *Sveriges Geologiska Undersökning, Rapporter och Meddelanden* **128**, 26–41.

Bergström, S.M. and Carnes, J.B. 1976 Conodont biostratigraphy and paleoecology of the Holston Formation (Middle Ordovician) and associated strata in eastern Tennessee, 27–57. In C.R. Barnes (ed.), *Conodont paleoecology*. The Geological Association of Canada, Special Paper **15**.

Bergström, S.M. and Ferretti., A. 2018 Deciphering the geology of some Darriwilian-Sandbian (Ordovician) 'ghost' formations in the UK and North America using olistoliths in marine debris flows. *Geological Magazine* **155**, 1507–22.

Bergström, S.M. and Orchard, M.J. (with contributions from Sevastopulo, G.D., Higgins, A.C., Savage, N.M., Aldridge, R.J., Brasier, M.D. and Rushton, A.W.A.) 1985 Conodonts of the Cambrian and Ordovician systems from the British Isles, 32–67. In A.C. Higgins and R.L. Austin (eds), *A stratigraphical index of conodonts*. British Micropalaeontological Society series. Ellis Horwood, Chichester, 263pp.

Bergström, S.M., Riva, J. and Kay, M. 1974 Significance of conodonts, graptolites, and shelly faunas from the Ordovician of Western and North-Central Newfoundland. *Canadian Journal of Earth Sciences* **11**, 1625–60.

Bergström, S.M., Chen, X., Gutierrez-Marco, J.C. and Dronov, A. 2009 The new chronostratigraphic classification of the Ordovician System and its relations to major regional series and stages and to $\delta^{13}C$ chemostratigraphy. *Lethaia* **42**, 97–107.

Blackwood, R.F. 1977 Northeastern Gander Zone, Newfoundland, 72–9. In R.V. Gibbons (ed.), *Report of Activities for 1977*. Newfoundland Department of Mines and Energy, Mineral Development Division, Report 78-1.

Bischoff, G.C.O. and Sanneman, D. 1958 Unterdevonische Conodonten aus dem Frankenwald. *Notizblatt des hessischen Landesamtes für Bodenforschung* **86**, 87–110.

Boyce, W.D., Ash, J.S., O'Neill, P. and Knight, I. 1988 Ordovician biostratigraphic studies in the Central Mobile Belt and their implications for Newfoundland tectonics, 177–82. In R.V. Gibbons (ed.), *Current Research 1988*. Newfoundland Department of Mines, Mineral Development Division, Report 88-1.

Branson, E.B. and Mehl, M.G. 1933 Conodonts from the Maquoketa-Thebes (Upper Ordovician) of Missouri. *University of Missouri Studies* **8**, 121–32.

Brenchley, P.J., Harper, J.C., Mitchell, W.I. and Romano, M. 1977 A reappraisal of some Ordovician successions in eastern Ireland. *Proceedings of the Royal Irish Academy* **B77**, 65–85, https://www.jstor.org/stable/ 20494273

Carlisle, H. 1979. Ordovician stratigraphy of the Tramore area, County Waterford, with a revised Ordovician correlation for south-east Ireland. *Geological Society, London*, *Special Publications* **8**, 545–54, https://doi.org/ 10.1144/GSL.SP.1979.008.01.65

Clark, D.L., Sweet, W.C. and Bergström, S.M. 1981 *Treatise on Invertebrate Paleontology W: Miscellanea, supplement 2: Conodonts*. Geological Society of America and University of Kansas Press, Lawrence, 202pp.

Cocks, L.R.M. and Torsvik, T.H. 2002 Earth geography from 500 to 400 million years ago: a faunal and palaeomagnetic review. *Journal of the Geological Society London* **159**, 631–44.

Cocks, L.R.M. and Torsvik, T. 2005 Baltica from the late Precambrian to mid-Palaeozoic times: the gain and loss of a terrane's identity. *Earth-Sciences Reviews* **72**, 39–66.

Cocks, L.R.M. and Torsvik, T. 2006 European geography in a global context from the Vendian to the end of the Palaeozoic, 83–95. In D.G. Gee and R.A. Stephenson (eds.), *European Lithosphaere Dynamics*. Geological Society, London, Memoirs **32**.

Cocks, L.R.M. and Torsvik, T.H. 2021 Ordovician palaeogeography and climate change. *Gondwana Research* **100**, 53–72, https://doi.org/10.1016/j.gr.2020.09.008

Cooper, B.J. 1975 Multielement conodonts from the Brassfield Limestone (Silurian) of southern Ohio. *Journal of Paleontology* **49**, 984–1008.

Drygant, D.M. 1974 New Middle Ordovician Conodonts from the Northwestern Volhynia. *Paleontologicheskiy Sbornik (L'vov)* **11**, 54–58 (in Russian).

Dzik, J. 1976 Remarks on the evolution of Ordovician conodonts. *Acta Palaeontologica Polonica* **21**, 395–455.

Dzik, J. 1978 Conodont biostratigraphy and Paleogeographical relations of the Ordovician Mójcza Limestone (Holy Cross Mts, Poland). *Acta Palaeontologica Polonica* **23**, 51–69.

Dzik, J. 1983 Relationships between Ordovician Baltic and North American Midcontinent conodont faunas. *Fossils and Strata* **15**, 59–85.

Dzik, J. 1989. Conodont evolution in high latitudes of the Ordovician, 1–28. In W. Ziegler (ed.), *Papers on Ordovician to Triassic Conodonts*. 1st International Senckenberg Conference and 5th European Conodont Symposium (ECOS IV) Contributions III. Courier Forschungsinstitut Senckenberg Series 117.

Dzik, J. 1994 Conodonts of the Mójcza Limestone. *Palaeontologica Polonica* **53**, 43–128.

Epstein, A.G., Epstein, J.B. and Harris, L.D. 1977 Conodont color alteration – an index to organic metamorphism. *U.S. Geological Survey Professional Paper* **995**, 1–27.

Erdtmann, B.-D. 1971 Ordovician graptolite zones of western Newfoundland in relation to paleogeography of the North Atlantic. *Geological Society of America Bulletin* **82**, 1509–28.

Ethington, R.L. 1959 Conodonts of the Ordovician Galena Formation. *Journal of Paleontology* **33**, 257–92.

Ethington, R.L. and Clark, D.L. 1981 Lower and Middle Ordovician conodonts from the Ibex Area Western Millard County, Utah. *Brigham Young University Geology Studies* **28**, 160pp.

Fåhræus, L.E. 1966 Lower Viruan (Middle Ordovician) conodonts from the Gullhögen quarry, southern central Sweden. *Sveriges Geologiska Undersökning C610*, 1–40.

Fåhræus, L.E. and Hunter, D.R. 1981. Paleoecology of selected conodontophorid species from the Cobbs Arm Formation (Middle Ordovician), New World Island, north-central Newfoundland. *Canadian Journal of Earth Sciences* **18**, 1653–65.

Fåhræus, L.E. and Hunter, D.R. 1985a Simple-cone conodont taxa from the Cobbs Arm Limestone (Middle Ordovician), New World Island, Newfoundland. *Canadian Journal of Earth Sciences* **22**, 1171–82.

Fåhræus, L.E. and Hunter, D.R. 1985b The curvature-transition series: integral part of some simple-cone conodont apparatuses (Panderodontacea, Distacodontacea, Conodontata). *Acta Palaeontologica Polonica* **30**, 177–89.

Ferretti, A. and Bergström, S.M. 2022 Middle–Upper Ordovician conodonts from the Ffairfach and Golden Grove groups in South Wales, United Kingdom. *Historical Biology* **34**, 462–85.

Ferretti, A., Bergström, S.M. and Sevastopulo, G.D. 2014 Katian conodonts from the Portrane Limestone: the first Ordovician conodont fauna described from Ireland. *Bollettino della Società Paleontologica Italiana* **53**, 105–19.

Fortey, R.A., Heward, A.P. and Miller, C.G. 2011 Sedimentary facies and trilobite and conodont faunas of the Ordovician Rann Formation, Ras al Khaimah, United Arab Emirates. *GeoArabia* **16**, 127–52.

Goldman, D., Sadler, P.M. and Leslie, S.A. 2020 The Ordovician Period, 631–94. In F. Gradstein, J.G. Ogg, M.D. Schmitz and G.M. Ogg (eds), *The Geologic Time Scale 2020*. Elsevier, https://doi.org/ 10.1016/B978-0-12-824360-2.00020-6

Goldman, D. Leslie, S.A., Liang, Y., and Bergström, S.M. 2023 Ordovician biostratigraphy: index fossils, biozones and correlation. 31–62. In D.A.T. Harper, B. Lefebvre, I.G. Percival and T. Servais (eds), A Global Synthesis of the Ordovician System: Part 1. Geological Society, London, Special Publications, 532.

Hadding, A. 1913 Undre dicellograptusskiffern i Skåne jämte några därmed ekvivalenta bildningar. *Lunds Universitets Årsskrift*, *N.F.*, Afd. 2, 9, 15, 1–91.

Hamar, G. 1964 The Middle Ordovician of the Oslo region, Norway. 17. Conodonts from the lower Middle Ordovician of Ringerike. *Norsk Geologisk Tidsskrift* **44**, 243–92.

Hamar G. 1966 The Middle Ordovician of the Oslo Region, Norway. 22. Preliminary report on conodonts from the Oslo-Asker and Ringerike districts. *Norsk Geologisk Tidsskrift* **46**, 27–83.

Hammer, Ø. 2023 *PAST. Paleontological Statistics, Version 4.14, Reference Manual*, Natural History Museum, University of Oslo, 311pp.

Hammer, Ø. and Harper, D.A.T. 2024 *Paleontological Data Analysis. 2nd Edition*. John Wiley and Sons.

Hammer, Ø., Harper, D.A.T. and Ryan, P.D. 2001 PAST: Paleontological statistics software package for education and data analysis. *Palaeontologica Electronica* **4**, 1–9. http://palaeo-electronica.org/2001_1/past/issue1_01.htm.

Harper, D.A.T. 1999 *Numerical Palaeobiology*. John Wiley and Sons.

Harper, D.A.T. 2023 The Irish Ordovician brachiopod fauna: A taxonomic renaissance, *Estonian Journal of Earth Sciences* **72**, 38–41.

Harper, D.A.T. and Parkes, M.A. 1989 Palaeontological constraints on the definition and development of the Irish Caledonide terranes. *Journal of the Geological Society*, *London* ***146***, 413–5, https://doi.org/10.1144/gsjgs.146.3.0413

Harper, D.A.T. and Parkes, M.A. 2000 *Ireland*. Geological Society, London, Special Reports 24, 52–64, https:// doi.org/10.1144/SR24.13

Harper, D.A.T., Parkes, M.A., Höey, A.N. and Murphy, F.C. 1990 Intra-Iapetus brachiopods from the Ordovician of eastern Ireland: implications for Caledonide correlation. *Canadian Journal of Earth Sciences* **27**, 1757–61, https://doi.org/10.1139/e90-181

Harper, D.A.T., Rasmussen, C.M.Ø., Liljeroth, M., Blodgett, R.B., Candela, Y., Jin, J. *et al.* 2013 Biodiversity, biogeography and phylogeography of Ordovician rhynchonelliform brachiopods. *Geological Society, London, Memoirs* **38**, 127–44.

Harper, J.C. and Rast, N. 1964 The faunal succession and volcanic rocks of the Ordovician near Bellewstown, Co. Meath. *Proceedings of the Royal Irish Academy* **B64**, 1–23, https://www.jstor.org/stable/20494877

Heredia, S. 1998 *Eoplacognathus robustus* (Conodonta) en la Formación Ponón Trehué (Ordovícico Inferior), Sierra Pintada, provincia de Mendoza, Argentina. *Ameghiniana* **35**, 337–44.

Heredia, S. and Mestre, A. 2015 The Balognathiid Ordovician conodonts *Eoplacognathus robustus* Bergström and *E. lindstroemi* Bergström. *Stratigraphy* **12**, 31–3.

Heredia, S. and Mestre, A. 2019 The Middle Ordovician conodonts *Eoplacognathus robustus* Bergström and *E. lindstroemi* (Hamar): taxonomy and apparatus reconstruction. *Andean Geology* **46**, 556–66.

Heredia, S. Mestre, A., Kaufmann, C. and Soria, T. 2019 Conodont biostratigraphy and depositional history of the Darriwilian (Middle Ordovician) *Pygodus serra* Zone, western Argentina. *Andean Geology* **46**, 336–44.

Heward, A.P., Booth, G.A., Fortey, R.A., Miller, C.G. and Sansom, I.J. 2018 Darriwilian shallow-marine deposits from the Sultanate of Oman, a poorly known portion of the Arabian margin of Gondwana. *Geological Magazine* **155**, 59–84.

Heward, A.P., Fortey, R.A., Miller, C.C. and Booth, G.A. 2023 New Middle Ordovician (Darriwilian) faunas from The Sultanate of Oman. *Proceedings of the Geologists' Association* **134**(3), 251–68. https://doi,org/10.1016/j.pgeola.2023.02.004

Hinde, G.J. 1879 On conodonts from the Chazy and Cincinnati Group of the Cambro-Silurian and from the Hamilton and Genesee-Shale divisions of the Devonian, in Canada and the United States. *Quarterly Journal of the Geological Society of London* **33**, 351–69.

Hints, O., Viira, V. and Nõlvak, J. 2012 Darriwilian (Middle Ordovician) conodont biostratigraphy in NW Estonia. *Estonian Journal of Earth Sciences* **6**, 210–26.

Holmer, L.E., Popov, L.E., Lehnert, O. and Ghobadi Pour, M. 2015 Ordovician (Darriwilian–Sandbian) linguliform brachiopods from the southern Cuyania Terrane of West-Central Argentina. *Stratigraphy* **12**, 110–1.

Holmer, L.E., Popov, L.E., Lehnert, O. and Ghobadi Pour, M. 2016 Ordovician (Darriwilian, Sandbian) linguliform brachiopods form the southern Cuyania Terrane of west-central Argentina. *Australasian Palaeontological Memoirs* **49**, 31–50.

Jeppsson, L. 1983 Simple-cones studies: some provocative thoughts. *Fossils and Strata* **15**, 86.

Key, M.M., Wyse Jackson, P.N., Patterson, W.P. and Moore, M.D. 2005 Stable isotope evidence of diagenesis of the Ordovician Courtown and Tramore limestones, south-eastern Ireland. *Irish Journal of Earth Sciences* **23**, 25–38.

Knüpfer, J. 1967 Zur Fauna und Biostratigraphie des Ordoviziums (Gräfenthaler Schichten) in Thüringen. *Freib$erger Forschungshefte* **C220**, 1–119.

Lamond, A. and Lindström, M. 1957 Arenigian and Llandeilian Cherts identified in the Southern Uplands by means of Conodonts, etc. *Transactions of the Edinburgh Geological Society* **17**, 60–70.

Landing, E., Keppie, J.D., Keppie, D.F., Geyer, G. and Westrop, S.R. 2022 Greater Avalonia – latest Ediacaran–Ordovician 'peribaltic' terrane bounded by continental margin prisms ('Ganderia,' Harlech Dome, Meguma): review, tectonic implications, and paleogeography. *Earth-Science Reviews* **224**, 103863. https://doi.org/10.1016/j.earscirev.2021.103863

Lehnert, O., Hinz-Schallreuter, I. and Krueger, H.H. 1999a Paläozoische Conodontenfaunen aus eiszeitlichen Geschieben Norddeutschlands (I): Eine Middelordoviz-Fauna aus Rügen. *Natur und Mensch, Jahresmitteilungen 1998*, 29–44.

Lehnert, O., Bergström, S.M., Keller, M. and Bordonaro, O. 1999b Middle Ordovician (Darriwilian-Caradocian) conodonts from the San Rafael region, west-central Argentina: Biostratigraphic, paleoecologic and paleogeographic implications. *Bolletino della Societá Paleontologica Italiana* **37,** 199–214.

Leslie, S.A. 2000 Mohawkian (Upper Ordovician) conodonts of eastern North America and Baltoscandia. *Journal of Paleontology* **74**, 1122–47.

Leslie, S.A. and Bergström, S.M. 1995 Element morphology and taxonomic relationships of the Ordovician conodonts *Phragmodus primus* Branson and Mehl, 1933, the type species of *Phragmodus* Branson and Mehl, 1933, and *Phragmodus undatus* Branson and Mehl, 1933. *Journal of Paleontology* **69**, 967–74.

Liljeroth, M., Harper, D.A.T., Carlisle, H. and Nielsen, A.T. 2017 Ordovician rhynchonelliformean brachiopods from Co. Waterford, SE Ireland: palaeobiogeography of the Leinster Terrane. *Fossils and Strata* **62**, 1–164. https://doi.org/10.1002/9781119412595

Lindström, M. 1954 Conodonts from the lowermost Ordovician strata of south-central Sweden. *Geologiska Föreningens i Stockholms Förhandlingar* **76**, 517–604.

Lindström, M. 1955 The conodonts described by A.R. Hadding, 1913. *Journal of Paleontology* **29**, 105–11.

Lindström, M. 1971 Lower Ordovician conodonts of Europe. In W. Sweet and S.M. Bergström (eds), *Symposium on Conodont Biostratigraphy*. Geological Society of America Memoir **127**, 21–61

Löfgren, A. 1978 Arenigian and Llanvirnian conodonts from Jämtland, northern Sweden. *Fossils and Strata* **13**, 1–129.

Löfgren, A. and Tolmacheva, T. 2003 The occurrence of the conodont *Drepanodus arcuatus* Pander, 1856, and related species in the Ordovician of Baltoscandia. *Paläontologische Zeitschrift* **77**, 181–99.

Männik, P. and Viira, V. 2012 Ordovician conodont diversity in the northern Baltic. *Estonian Journal of Earth Sciences* **61**, 1–14.

McConnell, B. 2000 The Ordovician volcanic arc and marginal basin of Leinster. *Irish Journal of Earth Sciences* **18**, 41–9.

McConnell, B.J., Stillman, C.J. and Hertogen, J. 1991 An Ordovician basalt to peralkaline rhyolite fractionation series from Avoca, Ireland. *Journal of the Geological Society, London* **148**, 711–8. https://doi.org/10. 1144/gsjgs.148.4.0711

McConnell, B., Crowley, Q.G. and Riggs, N. 2010 Laurentian origin of the Ordovician Grangegeeth volcanic arc terrane, Ireland. *Journal of the Geological Society* **167**, 469–74. https://doi.org/10.1144/ 0016-76492009-139

McConnell, B., Parkes, M., Crowley, Q. and Rushton, A. 2015 No Exploits back-arc basin in the Iapetus Suture zone of Ireland. *Journal of the Geological Society* **172**, 740–7. https://doi.org/10.1144/jgs2015-044

McConnell, B., Riggs, N. and Fritschle, T. 2021 Tectonic history across the Iapetus suture zone in Ireland, 333–45. In J.B. Murphy, R.A. Strachan and C. Quesada (eds), *Pannotia to Pangaea: Neoproterozoic and Paleozoic Orogenic Cycles in the Circum-Atlantic Region*. Geological Society, London, Special Publications **503**. https://doi.org/10.1144/SP503-2019-233

Meidla, T., Ainsaaar, L. and Hints, O. 2014 The Ordovician System in Estonia, 116–22. In H. Bauert, O. Hints, T. Meidla and P. Männik (eds), *4th Annual Meeting of IGCP 591, The Early to Middle Paleozoic Revolution, Estonia*. 10–19 June 2014.

Meidla, T., Ainsaar, L., Hints, O. and Radzeviclus, S. 2023 Ordovician of the Eastern Baltic palaeobasin and the Tornquist Sea margin of Baltica, 317–43. In D.A.T. Harper, B. Lefebvre, I.G. Percival and T. Servais (eds), *A Global Synthesis of the Ordovician System: Part 1*. Geological Society, London, Special Publications **532**. https://doi.org/10.1144/SP532-2022-141

Mellgren J.I.S. 2010 A rare occurrence of serrate conodont elements of *Panderodus* Ethington in the Middle Ordovician 'Täljsten' interval at Kinnekulle, south Sweden. *GFF* **132**, 183–91.

Mellgren, J.I.S., Schmitz, B., Ainsaar, L., Kirsimäe, K. and Eriksson, M. 2012 Conodont dating of the Middle Ordovician breccia cap-rock limestone on Osmussaar Island, northwestern Estonia. *Estonian Journal of Earth Sciences* **61**, 133–48.

Miller, C.G., Heward, A.P., Mossoni, A. and Sansom, I.J. 2018 Two new early balognathid conodont genera from the Ordovician of Oman and comments on the early evolution of prioniodontid conodonts. *Journal of Systematic Palaeontology* **16**, 571–93.

Molyneux, S.J., Harper, D.A.T., Cooper, M.R., Hollis, S.P., Raine, R.J., Rushton, A. W.A., Smith, M.P., Stone, S., Williams, M., Woodcock, N.H. and Zalasiewicz J.A. 2023 A synopsis of the Ordovician System in its birthplace – Britain and Ireland. In D.A.T. Harper, B. Lefebvre, I.G. Percival and T. Servais (eds), *A Global Synthesis of the Ordovician System: Part 1*. Geological Society, London, Special Publications **532,** 191–266. https://doi.org/10.1144/SP532-2022-235

Moskalenko, T.A. 1983 Conodonts from the Middle and Upper Ordovician of the Siberian Platform. *Akademiy Nauk SSR, Sibirskoe Ordelinie, Trudy Instituta Geologii i Geofiziki* **137**, 1–143 (in Russian).

Murphy, R.C., Anderson, T.B., Daly, J.S., Galagher, V., Graham, J.R., Harper, D.A.T., Johnston, J.D., Kennan, P.S., Kennedy, M.J., Long, C.B., Morris, J.H., O'Keeffe, W.G., Parkes, M., Ryan, P.D., Sloan, R.J., Stillman, C.J., Tietzsch-Tyler, D., Todd, S.P. and Wrafter, J.P. 1991 An appraisal of Caledonian suspect terranes in Ireland. *Irish Journal of Earth Sciences* **11**, 11–41.

Nielsen, A.T., Ahlberg, P., Ebbestad, J.O.R., Hammer, Ø., Harper, D.A.T., Lindskog, A., Rasmussen, C.M.Ø. and Stouge, S. 2023 A revised regional stage classification for the Ordovician of Scandinavia. In D.A.T. Harper, B. Lefebvre, I.G. Percival and T. Servais (eds), *A Global Synthesis of the Ordovician System: Part 1*. Geological Society, London, Special Publications **532**, 267–315.

Nowlan G.S. 1981 Some Ordovician conodont faunules from the Miramichi Anticlinorium, New Brunswick. *Geological Survey of Canada Bulletin* **345**, 1–35.

Nowlan, G.S. and Neuman, R.B. 1995 Paleontological contributions to Paleozoic paleogeographic and tectonic reconstructions. In H. Williams (ed.), *Geology of the Appalachian–Caledonian orogen in Canada and Greenland*. Geological Survey of Canada, Geology of Canada 6, 815–42.

Paiste, T., Männik, P. and Meidla, T. 2022 Sandbian (Late Ordovician) conodonts in Estonia: distribution and. biostratigraphy. *GFF* **144***,* 9–23.

Pander, C.H. 1856 *Monographie der fossilen Fische des Silurischen Systems der russisch-baltischen Gouvernements*. Buchdruckeri der Kaiserlichen Akademie der Wissenschaften, St. Petersburg, 91pp.

Parkes, M.A. and Harper, D.A.T. 1996 Ordovician brachiopod biogeography in the Iapetus suture zone of Ireland: provincial dynamics in a changing ocean. In P. Copper and J. Jin (eds), *Brachiopods: proceedings of the third international brachiopod congress*. Ba1kema, Rotterdam, 197–202.

Purnell, M.A., Donoghue, P.C.J. and Aldrigde, R.J. 2000 Orientation and anatomical notation in conodonts. *Journal of Paleontology* **74**, 113–22.

Rasmussen, J.A. 2001 Conodont biostratigraphy and taxonomy of the Ordovician shelf margin deposits in the Scandinavian Caledonides. *Fossils and Strata* **48**, 1–180.

Rasmussen, J.A. and Stouge, S. 1993 Late Arenig-early Llanvirn conodont biofacies across the Iapetus ocean. In J.D. Cooper, M.I. Droser and S.C. Finney (eds), *Ordovician Odyssey: Short Papers for the 7th International Symposium on the Ordovician System*. SEPM Pacific Section, Fullerton, California, Book 77, 443–7.

Rasmussen, J.A. and Stouge, S. 2018 Baltoscandian conodont biofacies fluctuations and their link to Middle Ordovician (Darriwilian) global cooling. *Palaeontology* **61**, 391–416.

Rejebian, V.A., Harris, A.G. and Huebner, J.S. 1987 Conodont color and textural variation: an index to regional metamorphism, contact metamorphism, and hydrothermal alteration. *Bulletin of the Geological Society of America* **99**, 471–9.

Rhodes, F.H.T. 1953 Some British Lower Palaeozoic conodont faunas. *Philosophical Transactions of the Royal Society of London, Series B* **237**, 261–334.

Ross, C.A. and Ross, J.R.P. 1995 North American depositional sequences and correlations. In J.D. Cooper, M.I. Droser and S.C. Finney (eds), *Ordovician Odyssey: Short Papers for the 7th International Symposium on the Ordovician System*. SEPM Pacific Section, Fullerton, California, Book 77, 309–13.

Sansom, I.J., Armstrong, H.A. and Smith, M.P. 1994 The apparatus architecture of *Panderodus* and its implications for coniform conodont classification. *Palaeontology* **37**, 781–99.

Sergeeva, S.P. 1963 Conodonts from the Lower Ordovician in the Leningrad region. *Akademia Nauk SSSR. Paleontologičeskij žurnal* **196**, 93–108, Moskva (in Russian).

Stauffer, C.R. 1930 Conodonts from the Decorah Shale. *Journal of Paleontology* **4**, 121–8.

Stauffer, C.R. 1935 Conodonts of the Glenwood beds. *Geological Society of America, Bulletin* **46**, 125–68.

Stauffer, C.R. 1940 Conodonts from the Devonian and associated days of Minnesota. *Journal of Paleontology* **14**, 417–35.

Stouge, S. 1980a Conodonts from the Davidsville Group, northwestern Newfoundland. *Canadian Journal of Earth Sciences* **17**, 268–72.

Stouge, S. 1980b Lower and Middle Ordovician conodonts from central Newfoundland and their correlatives in western Newfoundland. In C.F. O'Driscoll and R.Y. Gibbons (eds), *Current research*. Newfoundland Department of Mines and Energy. Mineral Development Division. Report **80-1**, 134–42.

Stouge, S. 1984 Conodonts of the Middle Ordovician Table Head Formation, western Newfoundland. *Fossils and Stata* **16**, 1–145.

Stouge, S. and Bagnoli, G. 1999 The suprageneric classification of some Ordovician prioniodontid conodonts. *Bollettino della Società Paleontologica Italiana* **37**, 145–58.

Stouge, S., Harper, D.A.T., Sevastopulo, G.D., O'Mahony, D. and Murray, J. 2016a Lower and Middle Ordovician conodonts of Laurentian affinity from blocks of limestone in the Rosroe Formation, South Mayo Trough, western Ireland and their palaeogeographic implication. *Geological Journal* 51, 584–99. https://doi.org/10. 1002/gj.2659

Stouge, S., Bauert, G., Bauert, H., Nõlvak, J. and Rasmussen, J.A. 2016b Upper Middle to lower Upper Ordovician chitinozoans and conodonts from the Bliudziai-150 core, southern Lithuania. *Canadian Journal of Earth Sciences* **53**, 781–87. dx.doi.org./10.1139/cjes-2015-0205

Stouge, S. Bagnoli, G. and Rasmussen, J.A. 2020 Late Cambrian (Furongian) to Mid-Ordovician Euconodont Events on Baltica: Invasions and immigrations. *Palaeogeography, Palaeoclimatology & Palaeoecology* **549**, 109151.

Sweet, W.C. 1979 Late Ordovician conodonts and biostratigraphy of the western Midcontinent Province. *Brigham Young University Geology Studies* **26**, 45–88.

Sweet, W.C. 1981a Genus *Phragmodus* Branson and Mehl, 1933. In W. Ziegler (ed.), *Catalogue of Conodonts **IV**,* 245–270. E. Schweizerbart'sche Verlagsbuchhandlung, Stuttgart.

Sweet, W.C. 1981b Macromorphology of elements and apparatuses, 5–20. In R.A. Robison (ed.), *Treatise on Invertebrate Paleontology*, *Pt. W. Miscellanea, Supplement 2*, *Conodonta*. Geological Society of America and University of Kansas Press, Lawrence.

Sweet, W.C. 1988 *The Conodonta: Morphology, Taxonomy, Paleoecology and Evolutionary History of a Long-Extinct Animal Phylum*. Oxford Monographs on Geology and Geophysics **10**, 212pp.

Sweet, W.C. and Bergström, S.M. 1962 Conodonts from the Pratt Ferry Formation (Middle Ordovician) of Alabama. *Journal of Paleontology* **36**, 1214–52.

Sweet, W.C. and Bergström, S.M. 1984 Conodont provinces and biofacies of the Late Ordovician, 69–87. In D.L. Clark (ed.), *Conodont Biofacies and Provincialism*. The Geological Society of America, Special Paper **196**, 340pp.

Sweet, W.C. and Schönlaub, H.P. 1975 Conodonts of the genus *Oulodus* Branson and Mehl, 1933. *Geologica and Palaeontologica* **9**, 41–59.

Sweet, W.C., Ethington, R.L. and Barnes, C.R. 1971 North American Middle and Upper Ordovician conodont faunas. In W.C. Sweet and S.M. Bergström (eds), *Symposium on Conodont Biostratigraphy*. Geological. Society of America Memoir **127**, 163–93.

Todd, S.P., Murphy, F.C. and Kennan, P.S. 1991 On the trace of the Iapetus suture in Ireland and Britain. *Journal of the Geological Society, London* **148**, 869–80.

Tolmacheva, T. 2014 *Biostratigraphy and biogeography of the Ordovician conodonts from the western part of Central Asian Fold Belt.* Vsegei, Russia (in Russian), 1–263.

Tolmacheva, T.Y. and Degtyarev, K.E. 2022 Ordovician Paleogeography: the possibilities and Constraints of conodont-based biographic reconstructions. *Geotectonics* **56**, 679–98.

Tolmacheva, T., Zaitsev, A.V. and Alekseev, A.S. 2013 Middle and Upper Ordovician conodonts. Of the Moscow Syneclise: New data on stratigraphy of the borehole Gavrilov Yam-1 section. *Stratigraphy and Geological Correlation* **21**, 383–407.

van Staal, C.R., Barr, S.M. and Murphy, J.B. 2012 Provenance and tectonic evolution of Ganderia: constraints on the evolution of the Iapetus and Rheic oceans. *Geology* **40**, 987–90.

van Staal, C.R., Barr, S.M., Waldron, J.W.F., Schofield, D.I., Zagorevski, A. and White, C.E. 2021 Provenance and Paleozoic tectonic evolution of Ganderia and its relationships with Avalonia and Megumia in the Appalachian–Caledonide orogen. *Gondwana Research* **98**, 212–43. https://doi.org/10.1016/j.gr.2021.05.025

van Wamel, W.A. 1974 Conodont biostratigraphy of the Upper Cambrian and Lower Ordovician of north-western Öland, south-eastern Sweden. *Utrecht Micropaleontological Bulletin* **10**, 1–126.

Viira, V. 1972 On symmetry of some Middle Ordovician conodonts. *Geologica et Paleontologica* **6**, 45–9.

Viira, V. 1974 *Konodonty Ordovika Pribaltiki* (Ordovician conodonts of the East Baltic). Eesti NSV teaduste Akadeemia Instituudi, Valgus, Tallinn, 1–142.

Viira, V. 2008 Conodont biostratigraphy in the Middle–Upper Ordovician boundary beds in Estonia. *Estonian Journal of Earth Sciences* **57**, 23–38.

Viira, V. 2011 Lower and Middle Ordovician Conodonts from the subsurface of SE Estonia and adjacent Russia. *Estonian Journal of Earth Sciences* **60**, 1–21.

Viira, V., Löfgren, A., Mägi, S. and Wickström, J. 2001 An Early to Middle Ordovician succession of conodont faunas at Mäekalda, northern Estonia. *Geological Magazine* **138**, 699–718.

Wu, R-C., Stouge, S., Zhan, R-B., Liu, J-B. and Liang, Y. 2016a Conodont faunal dynamics across the Middle and Upper Ordovician boundary in the Yichang area, western Hubei Province, South China. *Canadian Journal of Earth Sciences* **53**, 1–9.

Wu , R-C, Calner, M. and Lehnert, O. 2016b. Integrated conodont biostratigraphy and carbon isotope chemostratigraphy in the Lower–Middle Ordovician of southern Sweden reveals a complete record of the MDICE. Geological Magazine 154 (2), 334–53.

Wyse Jackson, P.N., Buttler, C.J. and Key Jr., M.M. 2002 Palaeonvironmental interpretation of the Tramore Limestone Formation (Llandeilo, Ordovician) based on bryozoan colony form. In P.N. Wyse Jackson, C.J. Buttler and S. Jones (eds), *Bryozoan Studies 2001*, Swets and Zeitlinger, Lisse, 359–65.

Zhang, J.H. 1998a The Ordovician conodont genus *Pygodus.* In H. Szaniawski (ed.), *Proceedings of the Sixth European Conodont Symposium (ECOS VI)*. *Palaeontologia Polonica* **58**, 87–105.

Zhang, J.H. 1998b Middle Ordovician conodonts from the Atlantic Faunal Region and the evolution of key conodont genera. *Meddelanden från Stockholms Universitets institution för geologi och geokemi* **298**, 5–27.

Zhang, J.H. 1998c Conodonts from the Guniutan Formation (Llanvirnian) in Hubei and Hunan Provinces, south–central China. *Stockholm Contributions in Geology* **46**, 1–161.

SVEND STOUGE

Natural History Museum of Denmark,

University of Copenhagen,

Øster Farimagsgade 2B

Dk-1350 Copenhagen K, Denmark

Corresponding author: e-mail: svends@snm.ku.dk

DAVID A.T. HARPER

Palaeoecosystems Group,

Department of Earth Sciences,

Durham University,

Durham DHI 3LE, UK

MATTHEW A. PARKES†

Natural History Museum,

National Museum of Ireland,

Merrion Street,

Dublin D02 F627,

Ireland

† Deceased

Figures:

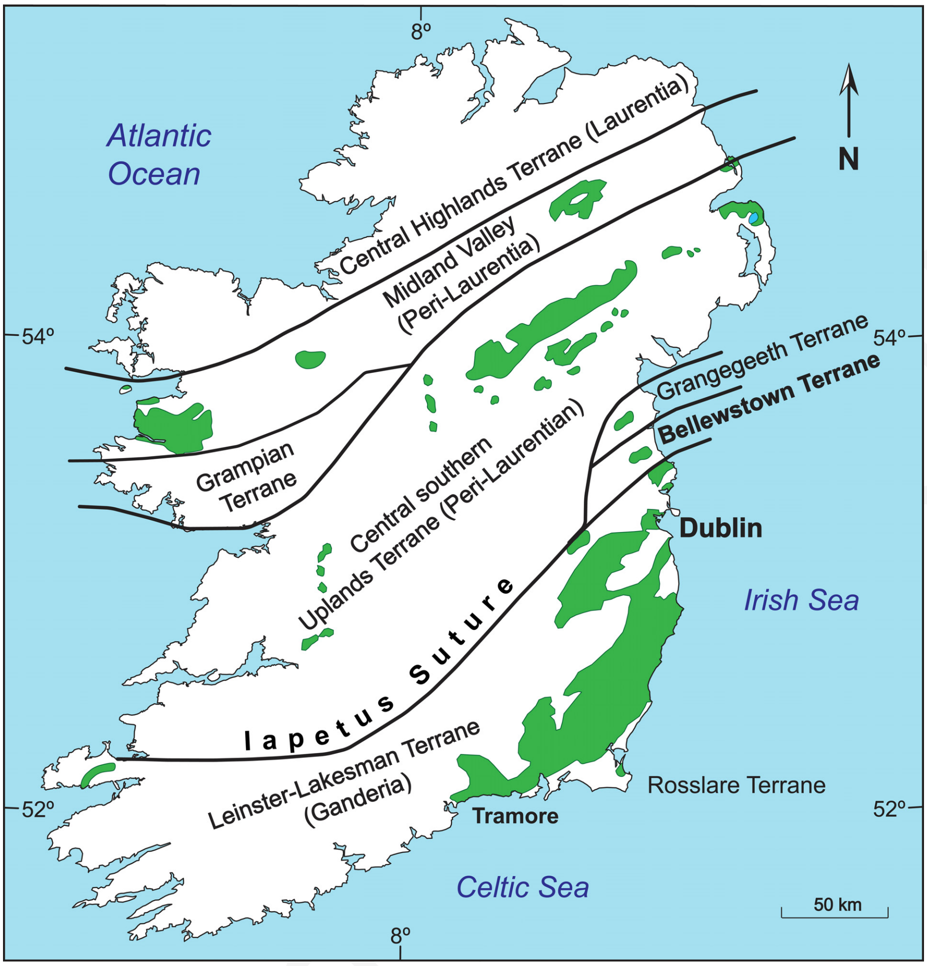

Fig. 1—Location map and approximate distribution of Ordovician rocks (green colour fill) in Ireland.

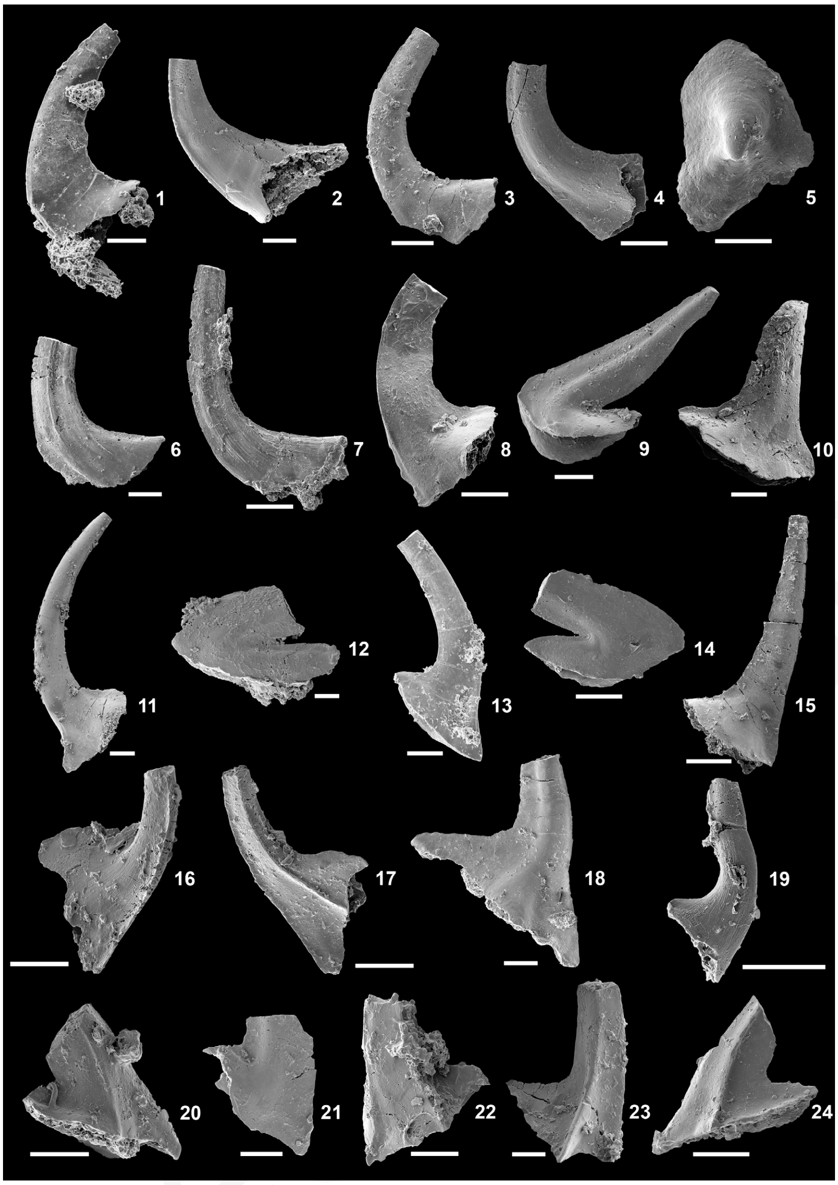

Fig. 2—SEM photos of conodont elements from the Bellewstown Limestone Member and Tramore Limestone Formation, in eastern and southeastern Ireland, respectively ~~(Plate 1)~~. **1–2**, Planoconvex elements of *Ansella* sp. in lateral view: 1, is sample Tram 14, No. TCD.65058 and 2, is sample BellEast 1, No. TCD.65059. **3–4**, Drepanodontiform elements of *Drepanodus* sp. in lateral view: 3 is sample Tram 14, No. TCD.65060, 4 is an inner lateral view of sample BellA 75, No. TCD.65061. **5**. *Pseudooneotodus mitratus* (Moskalenko, 1973) upper view: sample BellWest 1, No. TCD.65062. **6–7**, Lateral views of *Protopanderodus varicostatus* (Sweet and Bergström, 1962): 6 is sample Tram 10, No. TCD.65063 and 7 is sample BellEast 3, No. TCD.65064. **8–10**, *Drepanoistodus* sp. A: 8, drepanodontiform element, lateral view, sample BellEast 2, No. TCD.65065. 9, Oistodontiform element, lateral view, sample BellEast 7, No. TCD.65066. 10, Sub-erect drepanodontiform element in lateral view, sample BellEast 1, No. TCD.65067. **11–15**, *Drepanoistodus* sp. B: 11, Drepanodontiform element, lateral view, sample BellEast 4, No. TCD.65068. 12, Oistodontiform element, lateral view, sample BellEast 7, No. TCD.65069 13, Drepanodontiform element, lateral view, sample BellEast 7, No. TCD.65070. 14, Oistodontiform element, lateral view, sample BellN 75, No. TCD.65071. 15, Sub-erect drepanodontiform element, lateral view, sample Bell xxx, No. TCD.65072. **16–17**, Genus et sp. indet C: 16, Sc element, lateral view, sample BellEast 1, No. TCD.65073. 17, Sd element, lateral view, sample BellEast 3, No. TCD.65074. **18**, Pa element of *Triangulodus alatus* Dzik, 1976, lateral view, sample Tram 9, No. TCD.65075. **19**, Genus et sp. indet B striated and rounded simple cone; postero-lateral view, sample BellA 75, No. TCD.65076. **20–24**, Genus et sp. indet A: 20, Pa element, antero-lateral view, sample BellEast 3, No. TCD.65077. 21, M element, lateral view, sample BellEast 2, No. TDC.65078. 22, Sd element, inner lateral view, sample BellEast 3, No. TCD.65079. 23, Sd element, outer lateral view, sample BellEast 7, No. TCD.65080. 24. Pa element, outer lateral view, sample BellEast 3, No. TCD.65081.

Specimens 1,3, 6, 18 are from the Tramore Limestone Formation, specimens 2, 4, 5, 7–17, 19–24 are from the Bellewstown Limestone Member. Scale bars represent 100µm.

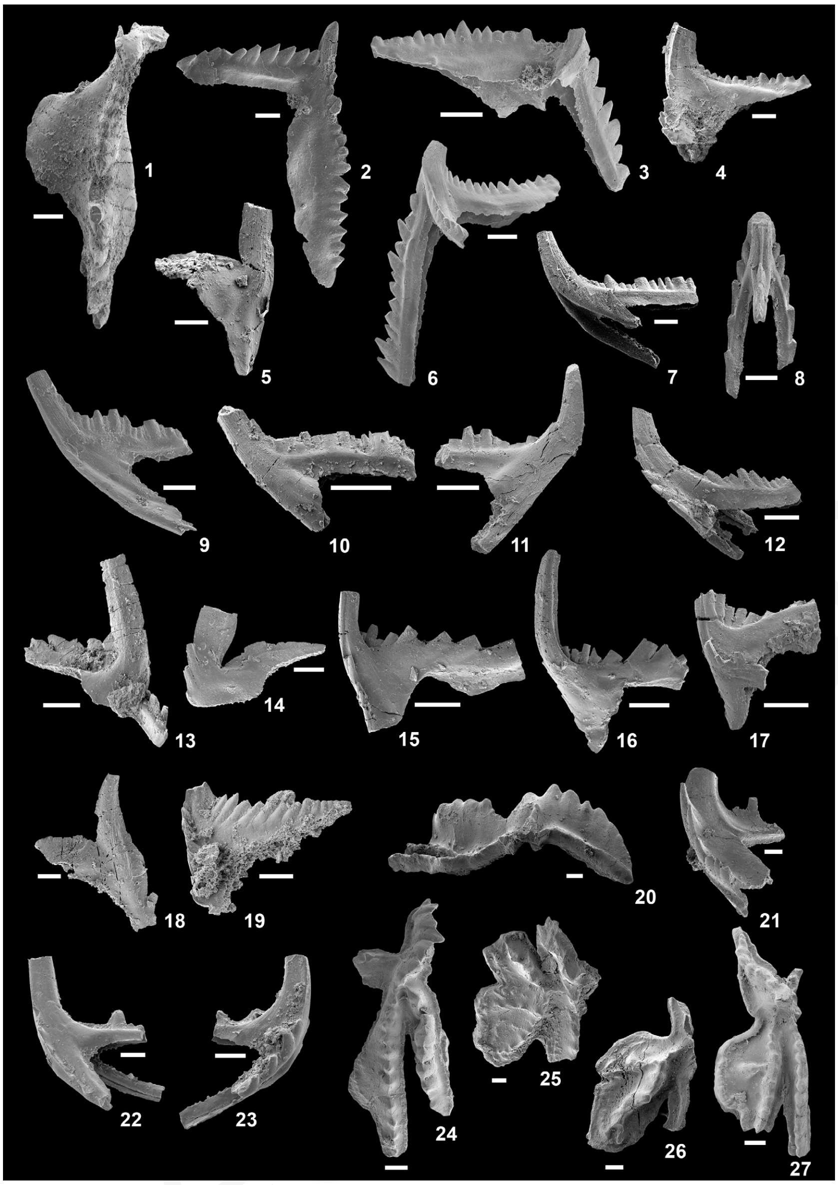

Fig. 3—SEM photos of conodont elements from the Bellewstown Limestone Member and Tramore Limestone Formation, in eastern and southeastern Ireland, respectively (Plate 2). **1–12**, *Baltoniodus alatus* (Hadding, 1913): 1, Pa element, upper view showing the large flare of the base, sample Tram 12, No. TCD.65082. 2, Pa element, posterior lateral view, distorted specimen, sample BellA 75, No. TCD.65083. 3, Pa element, lateral view, sample BellWest 14, No. TCD.65084. 4, Pb element, lateral view, sample BellWest 14, No. TCD.65085. 5, M element, inner lateral view, sample BellWest 14, No. TCD.65086 6, Pb element, antero-lateral view, sample BellWest 11, No. TCD.65087. 7, Sa element, antero-lateral view, sample BellWest 14, No. TCD.65088. 8, Sa element, posterior view, sample BellWest 14, No. TCD.65089. 9, Sb element, outer lateral view, sample BellWest 8, No. TCD.65090. 10, Sc element, outer lateral view, sample BellWest 15, No. TCD.65091. 11, Sc element, inner lateral view, sample BellWest 8, No. TCD.65092. 12, Sd element, inner lateral view, sample BellWest 15, No. TCD.65093. **13–17**, *Periodon aculeatus* Hadding, 1913: 13, Pa element, inner lateral view, sample Tram 9, No. TCD.65094. 14, M element, lateral view, sample BellWest 1, No. TCD.65095. 15, Sb element, inner lateral view, sample BellWest 8, No. TCD.65096. 16, Sc element, lateral view, Sample BellWest 8, No. TCD.65097. 17, Sd element, lateral view, sample BellWest 10, No. TCD.65098. **18–19**, *Pygodus serra* (Hadding, 1913): 18, M (falodontiform) element, lateral view, note denticulation on the anterior margin of the anti-cusp and the anterior bent of the tip of the cusp, sample BellWest 12, No. TCD.65099. 19, Pb (Haddingodontiform) element, lateral view, sample Tram 14, No. TCD.65100. **20–27**, *Sagittodontina sanrafaelensis* (Lehnert and Bergström, 1999): 20, Pa element, lateral view, sample BellWest 15, No. TCD.65101. 21, Pb element, antero-lateral view, sample BellWest 14, No. TCD.65102. 22, Sa element, lateral view, sample BellWest 12, No. TCD.65103. 23, Sb element, lateral view, sample BellWest 5, No. TCD.65104. 24, Pa (sinistral) element, upper view; fragment of mature specimen showing the development of the lateral flare, sample BellWest 16, No. TCD.65105. 25, Pa sinistral element, upper view, sample BellWest 15, No. TCD.65106. 26, Pa (dextral) element, upper view; fragment of mature specimen showing the large lateral flare; sample BellWest 12, No. TCD.65107. 27, Pa dextral element, upper view, sample BellWest 16, No. TCD.65108.

Specimens 1, 13, 19 are from the Tramore Limestone Formation, specimens 2–12, 14–18, 20–27 are from the Bellewstown Limestone Member. Scale bars represent 100µm.

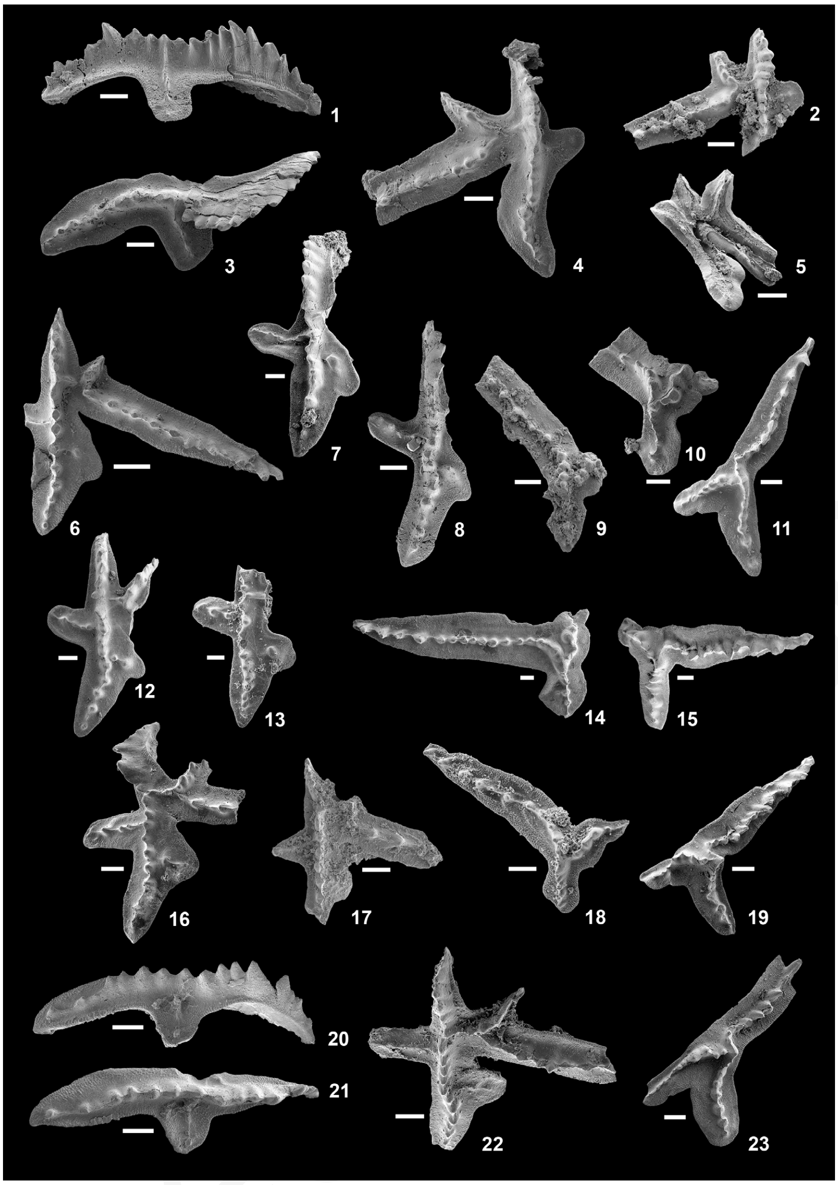

Fig. 4—SEM photos of conodont elements from the Bellewstown Limestone Member and Tramore Limestone Formation, in eastern and southeastern Ireland, respectively ~~(Plate 3)~~. **1–11**, *Eoplacognathus robustus* Bergström, 1971: 1, Sinistral Pa element, lateral view, sample BellWest 12, No. TCD.65109. 2, Sinistral Pa element, upper view, sample BellWest 13, No. TCD.65110. 3, Sinistral Pa element, upper view, sample BellN 75, No.TCD.65111. 4, Sinistral Pa element, upper view, sample BellN 75, No. TCD.65112. 5, Detail of Pa element, lower view showing the basal cavity, sample BellN 75, No. TCD.65113. 6, Dextral Pa element, upper view, sample BellWest 12, No. TCD.65114. 7, Dextral Pa element, upper view, sample BellN 75, No. TCD.65115. 8, Dextral Pa element, upper view, sample BellN 75, No. TCD.65116. 9, Sinistral Pb element, upper view, sample BellWest 13, No. TCD.65117. 10, Sinistral Pb element upper view, sample BellWest 12, No. TCD.65118. 11, Dextral Pb element, upper view, sample BellN 75, No. TCD.65119. **12–15**, *Eoplacognathus* cf. *E. robustus* Bergström, 1971: 12, Dextral Pa element, upper view, sample BellN 75, No. TCD.65120. 13, Dextral Pa element, upper view, sample Tram 14, ~~Bellewstown Limestone Member~~, No. TCD.65121. 14, Sinistral Pb element, upper view, note the angle of 90°, sample BellWest 12, No. TCD.65122. 15, Dextral Pb element, upper view, sample BellN 75, Bellewstown Limestone Member, No. TCD.65123. **16–23**, *Eoplacognathus reclinatus* (Fåhræus, 1966): 16, Dextral Pa element, upper view, sample BellWest 12, No. TCD.65124. 17, Dextral Pa element, upper view, sample Tram 14, upper view, No. TCD.65125. 18, Sinistral Pb element, upper view, sample BellN 75, No. TCD.65126. 19, Dextral Pb element, upper view, Sample BellN 75, No. TCD.65127. 20, Sinistral Pa element, lateral view, sample Bell West 12, No. TCD.65128. 21, Sinistral Pa element, upper view, sample BellN 75, No. TCD.65129. 22, Dextral Pa element, upper view, sample BellN 75, No. TCD.65130. 23, Dextral Pb element, upper view, sample BellN 75, No. TCD.65131.

Specimens 13, 17 are from the Tramore Limestone Formation, specimens 1–12, 14–16, 18–23 are from the Bellewstown Limestone Member. Scale bars represent 100µm.

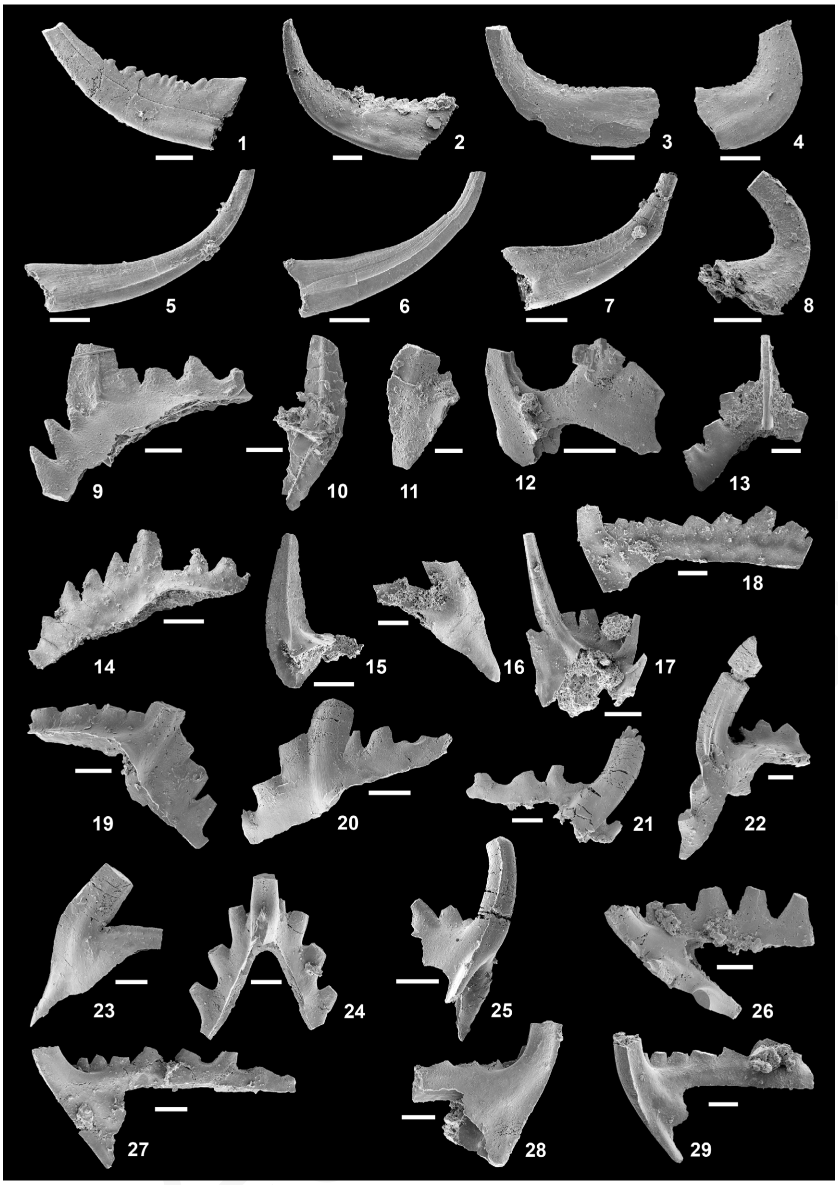

Fig. 5——SEM photos of conodont elements from the Bellewstown Limestone Member and Tramore Limestone Formation, in eastern and southeastern Ireland, respectively ~~(Plate 4)~~. **1–4**, *Belodella serrata* Dzik, 1976: 1, Biconvex specimen, lateral view, sample BellEast 7, No. TCD.65132. 2, Biconvex and lateral bent specimen, lateral view, Sample BellEast 7, No. TCD.65133. 3, Biconvex element, lateral view, sample BellN II, No TCD.65134. 4, Biconvex member with short base, sample BellN IV, No. TCD.65135. **5–8**, *Panderodus sulcatus* Fåhræus, 1966: 5, Slender element with costa, lateral view, sample BellEast 1, No. TCD.65136. 6, Slender element with costa and visible groove, sample BellEast 1, No. TCD.65137. 7, Planconvex slender element, lateral view, sample BellEast 1, No. TCD.65138. 8, Short base and recurved element, sample BellEast 4, No. TCD.65139. **9–12**, *Phragmodus polonicus* Dzik, 1978: 9, Pa element, lateral view, sample Tram 2, No. TCD.65140. 10, Pb element, lateral view, sample Tram 3, Tramore Limestone Formation, No. TCD.65141. 11, M element, lateral view, sample Tram 2, No. TCD.65142. 12, Sd element, lateral view, sample Tram 3, No. TCD.65143. **13–17**, *Plectodina* sp. A: 13, Sa element, posterior view, sample Tram 14, No. TCD.65144. 14, Pa element, inner lateral view, sample Tram 14, No. TCD.65145. 15, Pb element, inner lateral view, sample Tram 14, No. TCD.65146. 16, M element, lateral view, sample Tram 14, No. TCD.65147. 17, Sb element, inner lateral view, sample Tram 14, No. TCD.65148. 18, Sc element, inner lateral view, sample Tram 14, No. TCD.65149. **19–29**, *Plectodina* sp. B: 19, Pa element, inner lateral view, sample BellEast 2, No. TCD.65150. 20, Pa element, outer view, sample BellEast 2, No. TCD.65151. 21, Pb element, outer lateral view, sample BellEast 2, No. TCD.65152. 22, Pb element, inner lateral view, note repair of broken cusp, sample BellEast 7, No. TCD.65153. 23, M element, lateral view, sample BellEast 4, No. TCD.65154. 24, Sa element, posterior view, sample BellEast 7, No. TCD.65155. 25, Sb element, outer lateral view, sample BellEast 7, No. TCD.65156. 26, Sb element, inner lateral view, sample BellEast 3, No. TCD.65157. 27, Sc element, outer lateral view, sample BellEast 7, No. TCD.65158. 28, Sc element, inner lateral view, sample BellEast 4, No. TCD.65159. 29, Sd element, inner lateral view, with lateral costa, sample BellEast 7, No. TCD.65160.

Specimens 9–18 are from the Tramore Limestone Formation, specimens 1–8, 19–29 are from the Bellewstown Limestone Member. Scale bars represent 100µm.

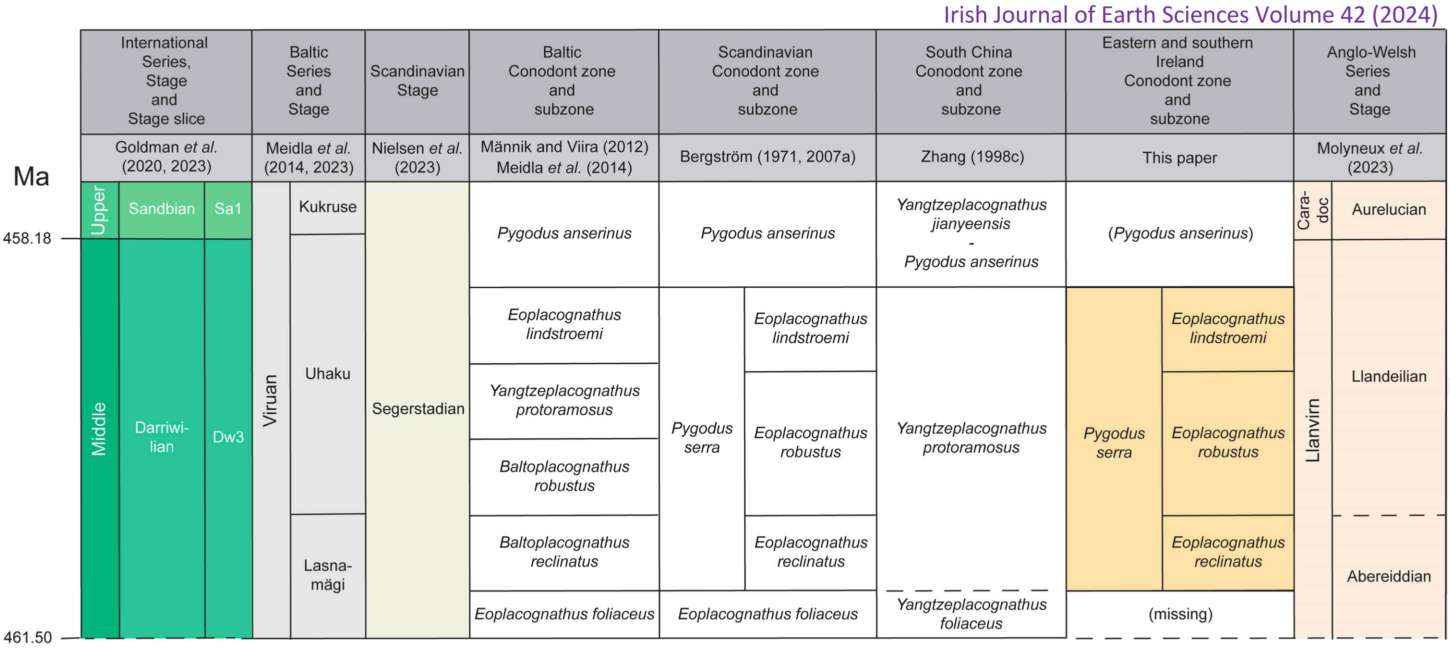

Fig. 6— Comparison and correlation of conodont zones and subzones through the Darriwilian Stage (Middle Ordovician).

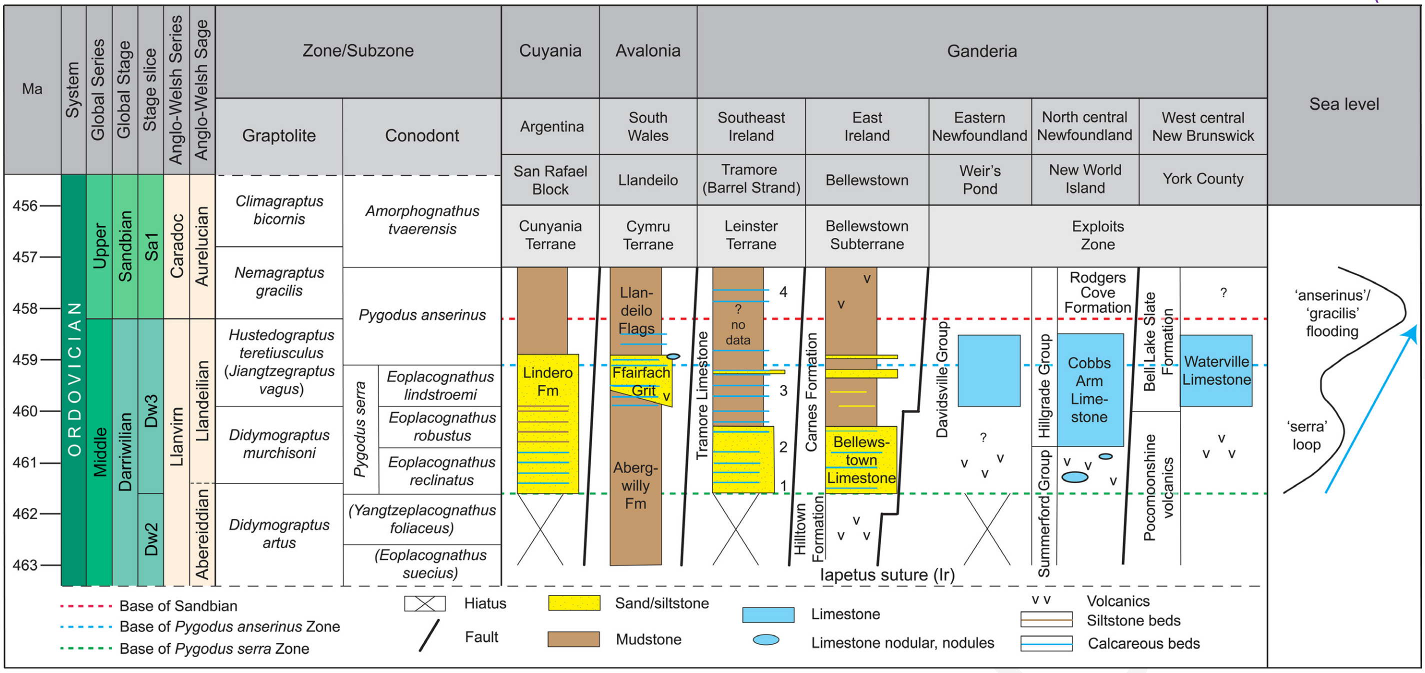

Fig. 7—Correlation of Bellewstown Limestone Member and Tramore Limestone Formation in Ireland with Darriwilian to Sandbian successions in South Wales, eastern Canada (New Brunswick), San Rafael Block of the Cuyania composite terrane, Mendoza Province, Argentina and the peri-Ganderian island arc rocks of central Newfoundland (Exploits Subzone).

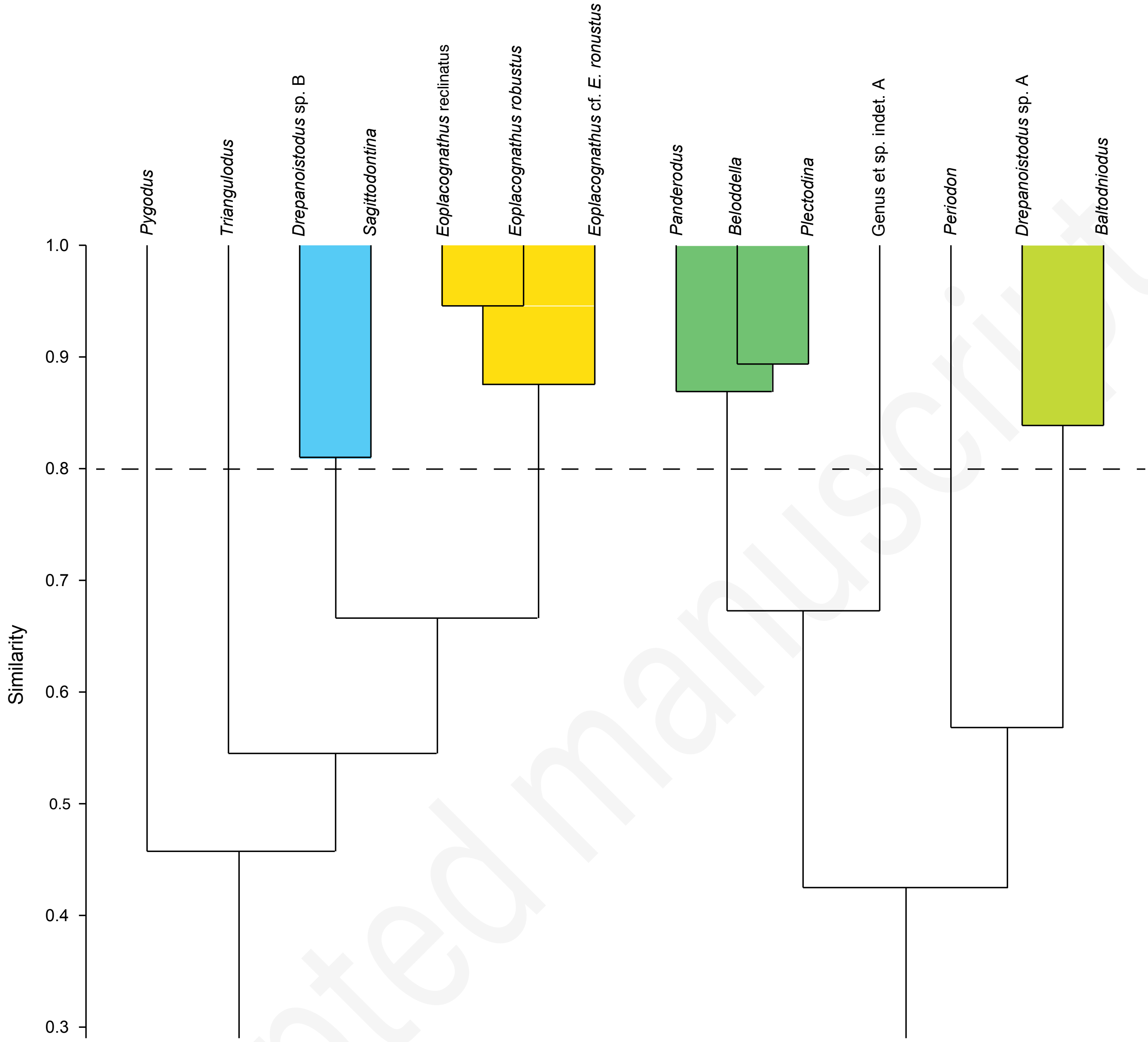

Fig. 8—R Mode normal cluster analysis (Morisita Similarity index) of the Bellewstown taxa and samples showing four taxa associations. The *Plectodina* and *Baltoniodus* associations represent the inner to mid shelf; the *Eoplacognathus* and *Sagittodontina* association represents the mid to outer shelf depositional environment.

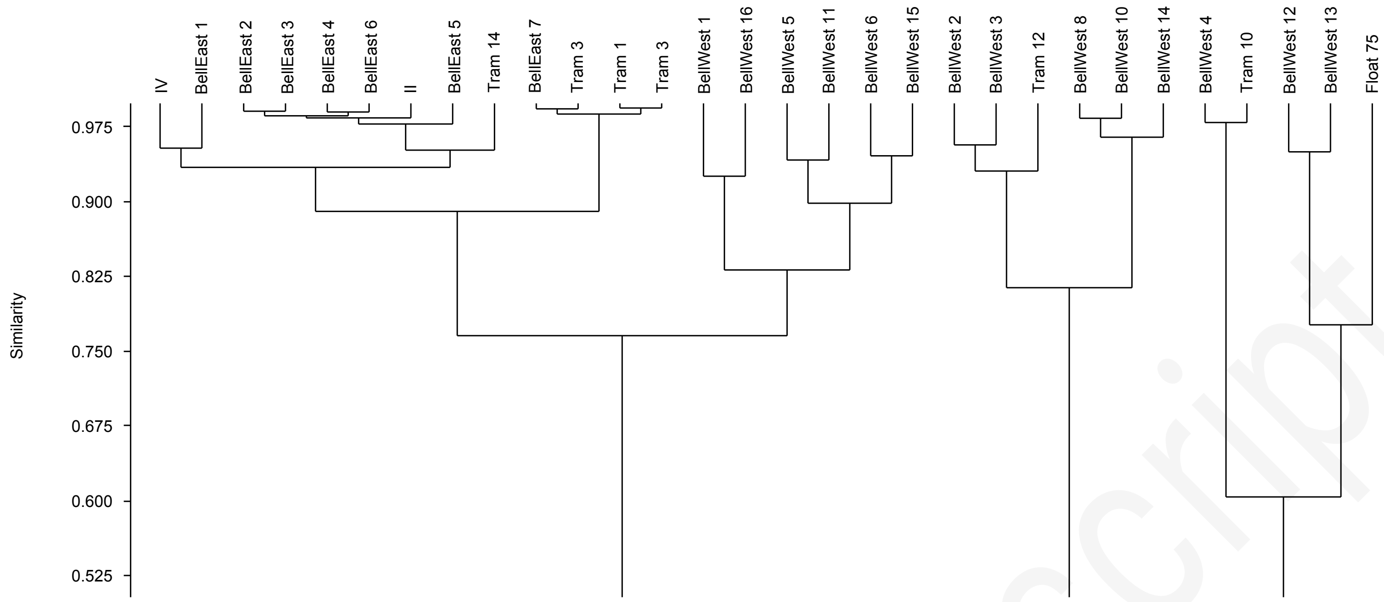

Fig. 9—Q Mode cluster analysis of the collected conodont specimens from the Tramore Limestone Formation and Bellewstown Limestone Member. The taxa associations evident in Fig. 8 are also evident here.

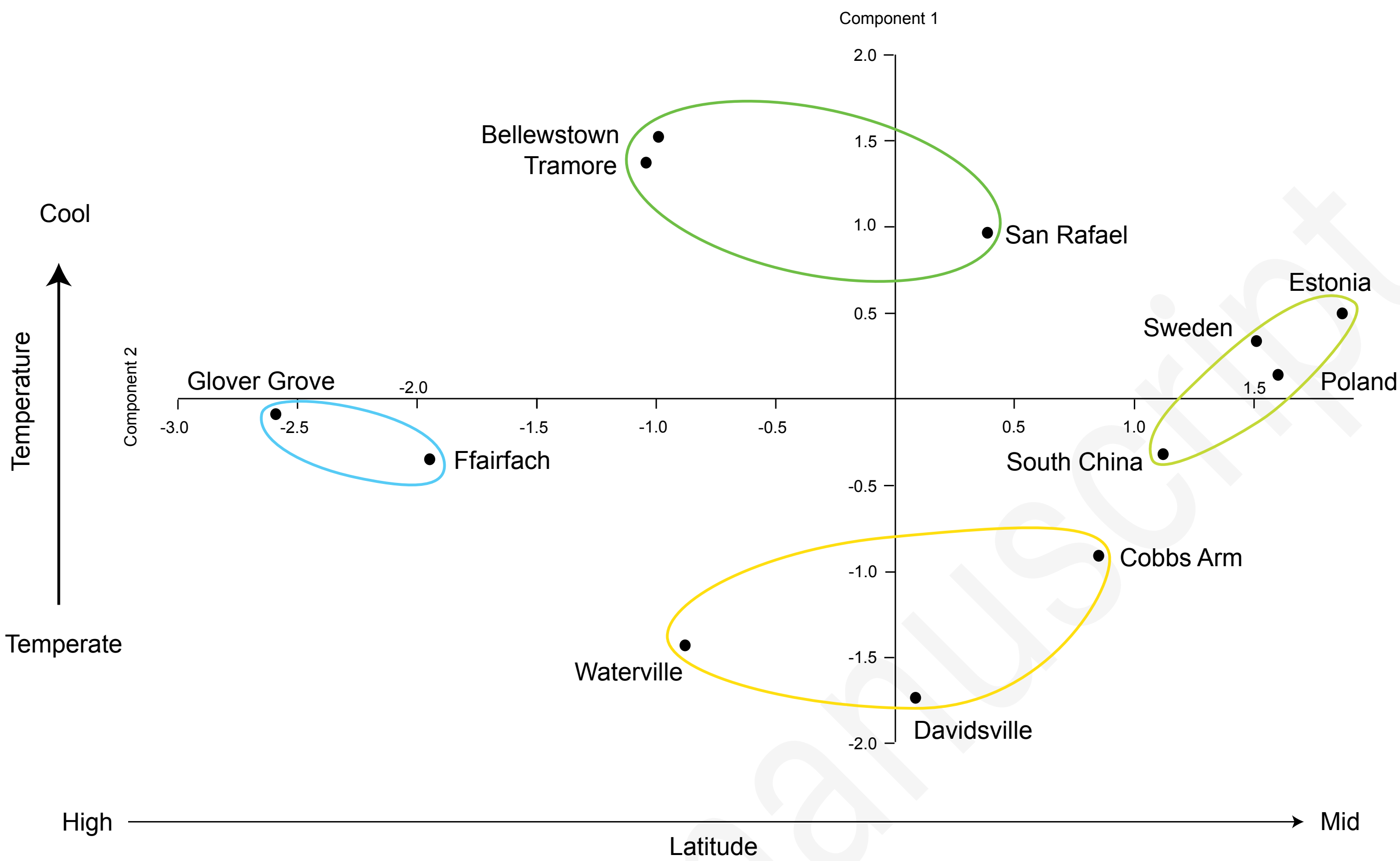

Fig. 10—Principal component analysis of Ireland, South Wales, New Brunswick, Canada), Cunyania composite terrane, Argentina, and the peri-Ganderian island arc rocks of central Newfoundland (Exploits Subzone; South Wales apparently was situated at the highest southern palaeolatitudinal position, South China and Baltica are closely related and probably occupied a similar latitudinal position. The Exploits Subzone is distinctly separate and clearly was not closely related to southern Ireland (cf. McConnell *et al.* 2015).

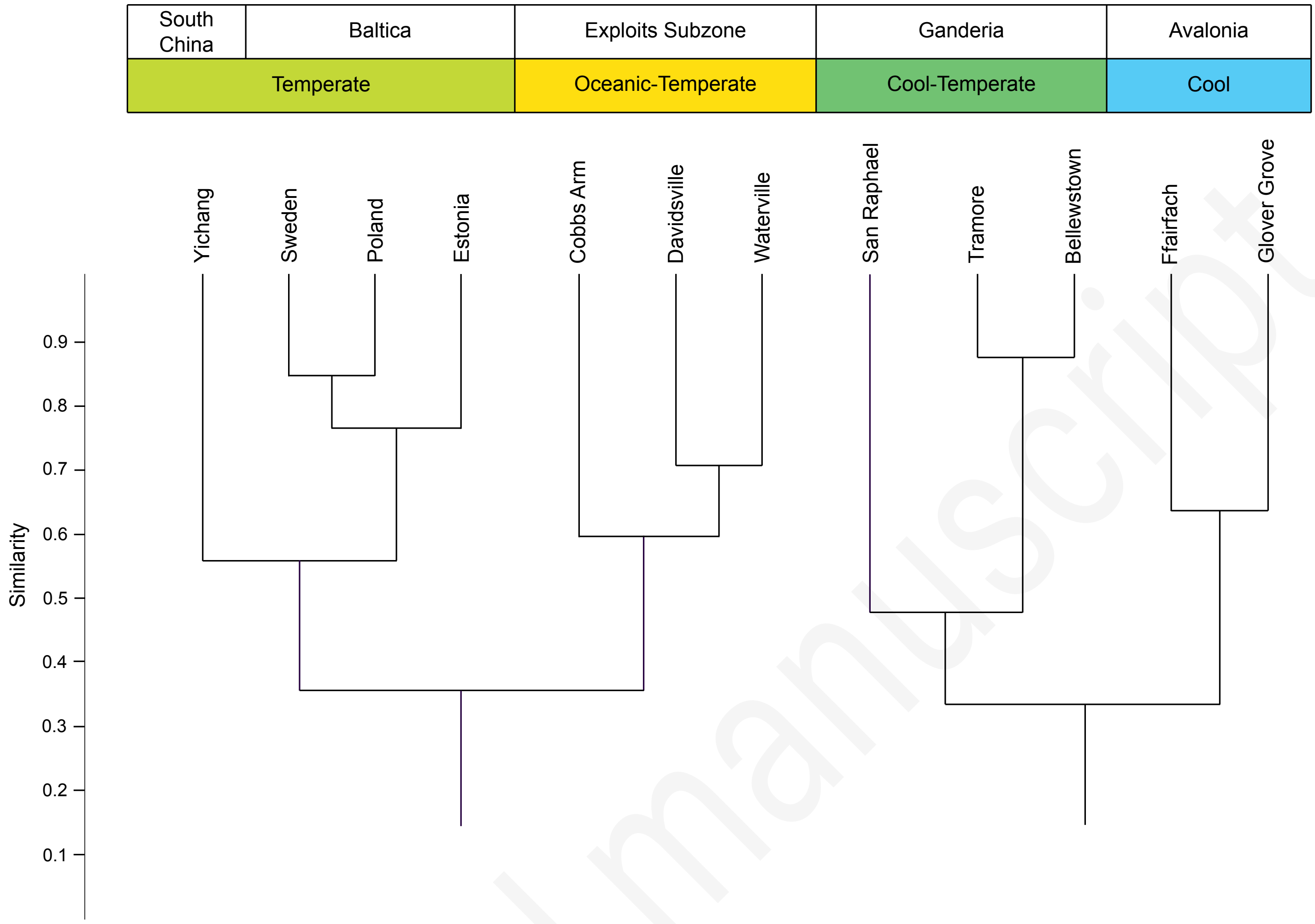

Fig. 11—Normal Cluster analysis (correlation similarity coefficient) of the Ganderia (Bellewstown (east Ireland), Tramore (southeast Ireland)), Cuyania (Mendoza, Argentina), Baltica (Sweden and Poland), Avalonia (South Wales) and South China Ordovician conodont faunas showing four distinct groups.

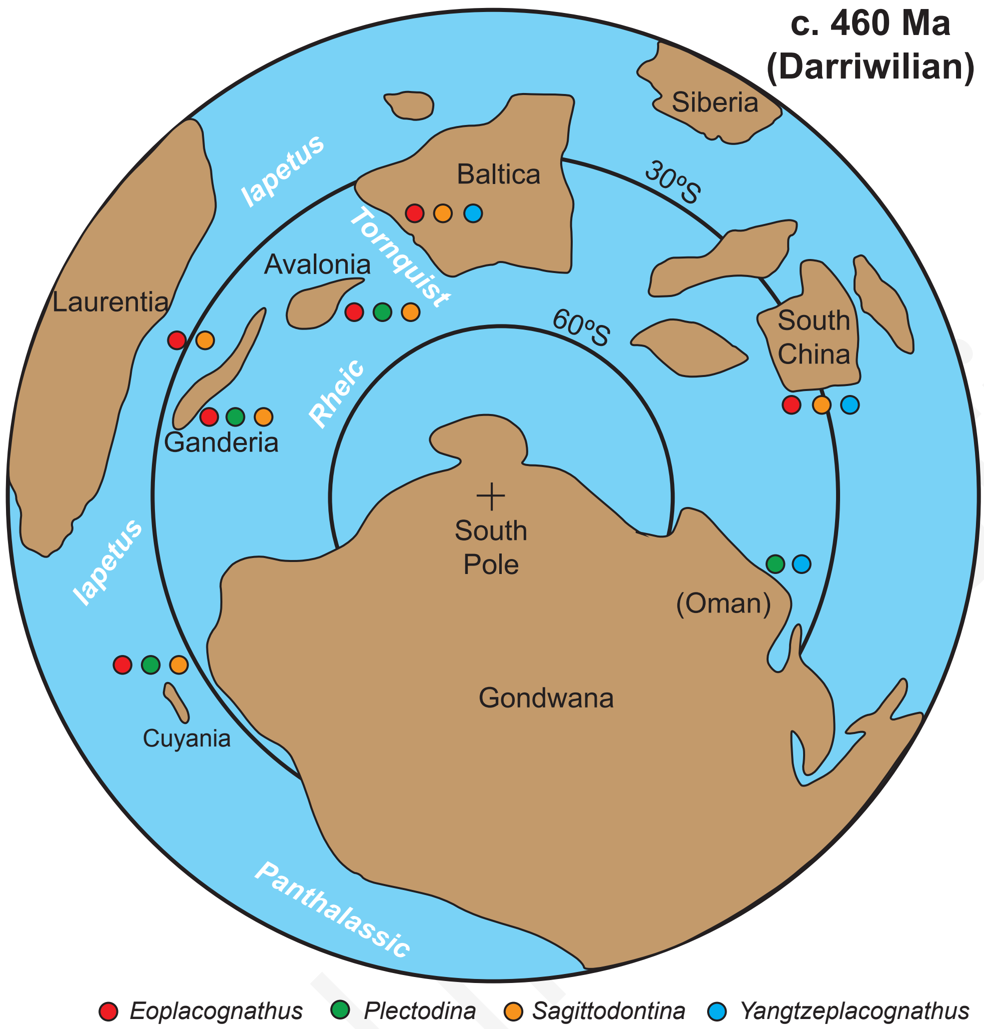

Fig. 12—Darriwilian palaeogeography and distribution of major palaeocontinents during the Darriwilian (Middle Ordovician), showing the known geographic distribution of *Eoplacognathus*, *Plectodina*, *Sagittodontina* and *Yangtzeplacognathus.* The taxa occupied a relatively cool to temperate climate zones on the palaeosouthern hemisphere. The genera are shared or have overlapping ranges on the eastern Cuyania Composite Terrane, Bellewstown (Ganderia), Tramore (Ganderia), Baltica, South Wales (Avalonia) and South China plates; coeval taxa of the Exploits Subzone of North America are assigned to the North Atlantic realm. The Arabian plate shares *Plectodina* and *Yangtzeplacognathus* (and possibly *Eoplacognathus*); however additional endemic genera from the Arabian plate define this region a distinct province.

Map based and simplified from Cocks and Torsvik (2005, 2006, 2021).

Table 1—Numerical distribution of conodonts in the Bellewstown East samples, eastern Ireland.

Table 1	Distribution of conodonts									
Bellewstown East										
Bellewstown Limestone Member										
CAI		**5**	**5**	**5**	**5**	5 to 6	5 to 6		elements	
Sample		BellEast 1	BellEast 2	BellEast 3	BellEast 4	BellEast 5	BellEast 6	BellEast 7	Total	Sum
Taxon										
Ansella sp.		1	0	0	0	0	0	0	1	1
Baltoniodus alatus										
	Pa	0	2	4	2	1	2	1	12	
	Pb	0	1	2	2	2	6	2	15	
	M	0	0	1	2	0	2	1	6	
	Sa	1	2	0	0	0	0	0	3	
	Sb	0	0	1	0	0	1	0	2	
	Sc	0	1	1	0	2	1	0	5	
	Sd	0	1	3	4	1	1	1	11	54
Belodella serrata		6	7	2	8	8	5	9	45	45
Drepanodus sp.		1	0	7	3	0	0	0	11	11
Drepanistodus sp.										
	Drepanodontiform	3	4	1	3	3	0	8	22	
	Suberectid	2	1	0	1	0	0	2	6	
	Oistodontiform	2	2	1	1	0	0	5	11	39
Drepanoistodus sp. B										
	Drepanoidontiform	0	0	6	7	4	2	4	23	
	Suberectid	0	0	1	0	0	2	0	3	
	Oistodontiform	1	0	1	1	0	1	3	7	33
Eopacognathus reclinatus										
	Pa	2	4	0	3	0	0	0	9	
	Pb	1	2	0	1	0	0	1	5	14
Eoplacognathus robustus										
	Pa	0	0	10	0	0	0	0	10	
	Pb	0	7	9	0	0	2	0	18	28
Eoplacognathus cf. *E. robustus*										
	Pa	0	0	0	3	0	4	0	7	
	Pb	0	7	0	6	0	3	0	16	23
Panderodus		40	29	35	62	38	38	22	264	264
Periodon aculeatus										
	Pa	0	0	0	0	0	0	1	1	
	Pb	0	0	0	0	0	0	1	1	
	M	0	0	2	0	0	0	5	7	
	S	0	0	0	0	0	1	1	2	11
Plectodina sp. B										
	Pa	9	7	5	18	10	7	19	75	
	Pb	4	16	21	16	13	12	38	120	
	M	7	12	12	22	10	8	10	81	
	Sa	11	17	24	20	15	11	41	139	
	Sb	4	7	13	8	5	8	17	62	
	Sc	17	25	47	42	21	32	65	249	
	Sd	4	7	7	16	2	7	17	60	786
Phragmodus polonicus										
	M	0	0	0	2	0	0	0	2	
	S	0	0	0	6	3	0	0	9	11
Protopanderodus varicostatus		0	0	1	0	0	0	0	1	1
Sagittodontina sanrafaelensis										
	Pa	0	0	4	2	1	0	0	7	
	Pb	0	2	1	1	0	0	1	5	
	M	0	1	0	1	0	0	0	2	
	Sa	0	0	0	1	1	1	0	3	
	Sb	0	0	0	0	1	0	0	1	
	Sc	0	0	0	2	0	0	0	2	
	Sd	0	1	0	2	0	0	0	3	23
Triangulodus alatus		2	0	0	3	3	0	0	8	8
Genus et sp. Indet A		1	4	10	0	6	0	6	27	27
Genus et sp. Indet B		1	4	0	0	0	0	0	5	5
Gen et sp. Indet C		2	3	3	1	0	0	0	9	9
Genus et sp. Indet.		0	6	3	2	5	6	4	26	26
Total		122	182	238	274	155	163	285	1419	1419

Table 2—Numerical distribution of conodonts in the Bellewstown West samples, eastern Ireland.

Table 2	Distribution of conodonts																	
Bellewstown Limestone Member	Bellewstown West																	
CAI		5	5 to 6	5	5	5	5	5	5	5	5	5	5	5	5	5		
Sample		BellWest 1	BellWest 2	BellWest 3	BellWest 4	BellWest 5	BellWest 6	BellWest 8	Sample 9	BellWest 10	BellWest 11	Sample 12	Sample 13	BellWest 14	BellWest 15	BellWest 16	Total	Sum
																	Elements	
Taxon																		
Baltoniodus alatus																		
	Pa	2	3	2	0	0	2	12	1	7	1	0	0	13	1	6	50	
	Pb	0	3	0	0	0	1	15	0	12	0	0	0	6	2	8	47	
	M	2	0	0	0	0	1	9	0	0	1	1	1	2	3	2	22	
	Sa	0	0	1	0	0	0	1	0	1	0	1	0	0	1	1	6	
	Sb	1	1	2	0	0	1	3	0	4	1	0	0	2	0	0	15	
	Sc	1	1	0	1	1	0	3	0	1	0	1	0	0	1	0	10	
	Sd	1	1	1	0	0	0	3	0	3	0	0	0	3	5	3	20	170
Belodella serrata		1	1	0	0	0	1	0	2	1	1	1	0	2	0	2	12	12
Drepanodus sp.		0	0	0	0	0	0	0	0	0	0	0	0	0	0	2	2	2
Drepanoistodus sp. A																		
	Drepanodontiform	1	0	3	0	0	0	12	2	6	4	0	6	10	0	5	49	
	Suberectid	1	0	0	0	0	0	3	0	1	0	0	0	7	0	1	13	
	Oistodontiform	1	1	0	0	0	0	5	2	4	1	0	1	4	0	3	22	84
Drepanoistodus sp. B																		
	Drepanodontiform	0	1	2	2	4	3	4	4	4	0	4	0	1	6	3	38	
	Suberectid	0	0	0	0	1	2	1	0	0	0	0	0	0	1	1	6	
	Oistodontiform	0	0	0	1	0	0	3	0	1	0	2	0	0	6	2	15	59
Eoplacognathus reclinatus																		
	Pa	1	2	1	1	0	0	0	0	0	0	10	0	0	0	0	15	
	Pb	0	0	0	2	0	0	0	0	0	0	10	2	0	1	0	15	30
Eoplacognathus robustus																		
	Pa	0	0	0	0	0	0	0	0	0	0	13	19	0	0	0	32	
	Pb	0	0	0	0	0	0	0	0	0	0	12	11	1	0	1	25	57
Eoplacognathus cf. *E. robustus*																		
	Pa	0	0	0	0	0	0	2	0	1	0	19	11	0	0	0	33	
	Pb	0	0	0	0	1	0	1	0	0	0	12	8	0	0	0	22	55
Panderodus sulcatus		3	1	1	0	1	2	5	1	1	2	5	4	5	5	9	45	45
Periodon aculeatus																		
	Pa	0	0	0	0	0	0	0	1	0	0	0	0	0	0	2	3	
	Pb	0	0	0	0	0	0	0	0	0	0	0	0	0	0	1	1	
	M	1	0	0	0	0	1	0	0	0	0	1	1	1	1	1	7	
	Sa	0	0	0	0	0	1	1	0	0	0	0	0	0	0	0	2	
	Sb	0	0	0	0	0	0	1	0	0	0	0	0	0	0	0	1	
	Sc	0	0	0	0	0	0	0	1	0	0	0	0	0	0	0	1	
	Sd	0	0	0	0	0	0	1	0	0	0	0	0	0	0	0	1	16
Plectodina sp. B																		
	Pa	1	0	0	0	0	0	2	0	3	1	1	0	0	7	3	18	
	Pb	3	1	0	0	1	1	2	0	4	2	0	1	5	1	5	26	
	M	1	0	0	1	2	0	2	0	0	0	0	1	1	2	6	16	
	Sa	0	3	1	1	1	3	5	0	1	0	6	2	5	4	9	41	
	Sb	2	0	1	1	0	1	0	1	0	1	1	0	2	1	2	13	
	Sc	2	5	1	0	2	2	15	0	6	3	2	2	8	7	14	69	
	Sd	2	1	0	0	0	0	2	0	1	0	0	0	0	2	1	9	192
Pseudooneotodus mitratus		1	0	0	0	0	0	0	0	0	0	0	0	0	0	0	1	1
Pygodus cf. *P. serra*												0						
	M	0	0	0	0	0	0	0	0	0	0	2	0	0	1	0	3	3
Sagittodontina sanrafaelensis																		
	Pa	0	0	1	0	0	1	0	0	0	0	2	2	0	6	3	15	
	Pb	0	0	0	0	1	1	1	0	3	0	2	0	0	0	2	10	
	M	0	0	0	0	1	0	0	0	0	0	0	1	0	0	0	2	
	Sa	0	0	0	0	0	0	0	0	0	0	0	0	0	0	1	1	
	Sb	0	0	0	0	1	0	0	0	0	0	0	0	0	1	0	2	
	Sc	0	0	0	0	0	0	0	0	0	0	0	0	0	0	0	0	30
Triangulodus alatus		0	0	0	0	0	2	0	0	0	0	1	1	4	1	1	10	10
Gen et sp. Indet A		0	0	0	0	0	0	0	0	0	0	0	0	0	1	1	2	2
Genus et sp. Indet D		0	0	0	0	0	0	0	1	1	0	0	0	0	0	3	5	5
																		773
Total		28	25	17	10	17	26	114	16	66	18	109	74	82	67	104	773	

Table 3—Numerical distribution of conodonts in the Bellewstown North samples, eastern Ireland.

Table 3	Distribution of conodonts									
Bellewstown Limestone Member										
CAI		5	5	5	5	5 to 6	5 t0 6	5		
Samples		I	II	IV	V	B	C	BellN 75	Total	Sum
Taxon									elements	
Baltoniodus alatus										
	Pa	0	2	0	0	0	1	4	7	
	Pb	0	1	0	0	4	2	4	11	
	M	0	1	0	0	1	5	1	8	
	Sa	0	2	0	0	0	0	2	4	
	Sb	0	0	0	0	1	1	1	3	
	Sc	1	0	0	0	2	1	1	5	
	Sd	0	0	0	0	0	2	1	3	41
Belodella serrata		1	3	3	0	1	5	3	16	16
Drepanodus arcuatus		0	0	0	0	0	2	1	3	3
Drepaniostodus sp. A										
	Drepanodontiform	1	0	0	0	2	3	0	6	
	Suberectid	0	0	0	0	2	1	0	3	
	Oistodontiform	0	0	0	0	3	3	0	6	15
Drepanistodus sp. B										
	Drepanodontiform	0	5	0	0	0	3	15	23	
	Suberectid	0	1	0	0	0	0	2	3	
	Oistodontiform	0	0	0	0	0	1	5	6	32
Eoplacognathus reclinatus										
	Pa	0	6	0	0	3	3	10	22	
	Pb	0	1	0	0	2	5	6	14	36
Eoplacognathus robustus										
	Pa	0	0	0	0	0	0	19	19	
	Pb	0	0	0	0	0	0	16	16	35
Eoplacognathus cf. *E. robustus*										
	Pa	0	2	0	0	0	1	23	26	
	Pb	0	3	0	0	0	1	33	37	63
Panderodus sulcatus		6	17	4	1	1	34	30	93	93
Periodon aculeatus										
	M	0	2	0	0	2	1	1	6	
	Sd	0	0	0	0	0	0	1	1	7
Plectodina sp. B										
	Pa	0	18	1	0	14	15	8	56	
	Pb	1	6	3	0	14	24	9	57	
	M	1	7	1	0	22	17	7	55	
	Sa	1	20	1	1	25	21	7	76	
	Sb	0	5	1	0	5	5	6	22	
	Sc	0	21	2	0	39	32	14	108	
	Sd	2	3	2	0	5	2	7	21	395
Pygodus cf. *P. serra*		0	0	0	0	0	0	2	2	2
Sagittodontus sanrafaelensis										
	Pa	0	0	0	0	1	1	1	3	
	Pb	0	0	0	0	0	3	4	7	
	M	0	0	0	0	1	0	0	1	
	Sa	0	0	0	0	0	0	1	1	
	Sb	0	0	0	0	1	0	3	4	
	Sc	0	0	0	0	2	0	1	3	19
Triangulodus alatus		0	0	0	0	0	0	4	4	4
Genus et sp. Indet A		0	0	0	0	4	6	3	13	13
Genus et sp. Indet B		1	0	0	0	0	1	1	3	3
Genus et sp. Indet C		0	0	0	0	1	0	1	2	2
Genus et sp. Indet		0	0	0	1	1	5	7	14	14
										793
Total		15	126	18	3	159	207	265	793	

Table 4—Numerical distribution of conodonts in the samples yielding conodonts from the Tramore Limestone Formation, southeastern Ireland.

Table 4	Distribution of conodonts										
Tramore											
Tramore Limestone Formation											
CAI		5	5	5	5	5-6	5-6	5-6.5	5-6.5		
Sample		Tram 1	Tram 2	Tram 3	Tram 4	Tram 5	Tram 10	Tram 12	Tram 14	Total	Sum
										Elements	
Taxon											
Baltoniodus alatus											
	Pa	0	0	0	0	0	0	2	0	2	
	Pb	0	0	0	0	0	0	1	0	1	
	M	0	0	0	0	0	1	1	0	2	
	Sc	0	0	0	0	0	0	1	0	1	
	Sd	0	0	0	0	0	0	1	1	2	8
Drepanodus sp.		0	0	0	0	0	0	0	1	1	1
Drepanoistodus sp. A											
	drepanodontiform	0	0	0	1	1	0	0	5	7	
	suberectiform	0	0	1	1	1	0	0	0	3	
	oistodontiform	0	0	0	0	0	0	0	1	1	11
Drepanoistodus sp. B											
	drepanodontiform	0	0	0	0	0	2	0	4	6	
	suberectiform	0	0	0	0	0	0	0	2	2	
	oistodontiform	0	0	0	0	0	0	0	3	3	11
Eoplacognathus reclinatus											
	Pa	0	0	0	0	0	1	0	11	12	
	Pb	2	1	1	1		1	0	2	8	20
Eoplacognathus robustus											
	Pa	0	0	0	0	0	0	1	3	4	
	Pb	0	0	0	0	0	0	0	1	1	5
Eoplacotnathus cf *E. robustus*											
	Pa	0	0	0	0	0	0	0	2	2	
	Pb	0	0	0	0	0	0	0	1	1	3
Panderodus		2	3	1	0	0	0	0	10	16	21
Periodon aculeatus											
	Pa	0	0	0	0	0	0	0	1	1	1
Phragmodus polonicus											
	Pa		1	0	0	0	0	0	0	1	
	Pb		2	1	0	0	0	0	0	3	
	M		1	1	0	0	0	0	0	2	
	Sa		1	0	0	0	0	0	0	1	
	Sd		0	1	0	0	0	0	0	1	8
Plectodina sp. A											
	Pa	2	7	3	0	0	0	1	37	50	
	Pb	1		1	1	0	0	0	3	7	
	M	5	9	3	1	1	0	0	7	26	
	Sa	2	3	1	0	0	0	0	4	10	
	Sb	2	0	0	0	0	0	0	1	3	
	Sc	6	11	2	0	0	0	0	3	22	
	Sd	1	0	1	0	1	0	1	0	4	122
Protopanderodus varicostatus		0	1	0	0	0	1	0	1	3	3
Pygodus cf. *P. serra*											
	Pb	0	0	0	0	0	0	0	1	1	
	M	0	0	0	0	0	0	0	2	2	3
Triangulodus alatus		0	0	0	0	0	0	0	1	1	1
Genus Indet A		0	0	0	0	0	0	0	1	1	1
Genus Indet B		0	0	0	0	0	3	0	4	7	7
Total		23	40	17	5	4	9	9	113	220	226